



Overview of the ALICE UPC experimental results



Adam Matyja

Institute of Nuclear Physics
Polish Academy of Sciences, Kraków

24th Zimanyi School Winter Workshop on Heavy Ion Physics

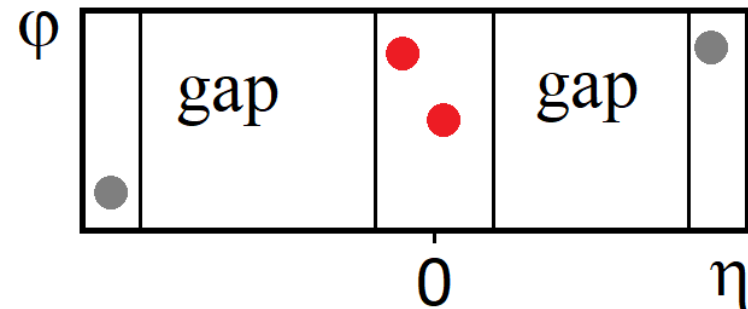
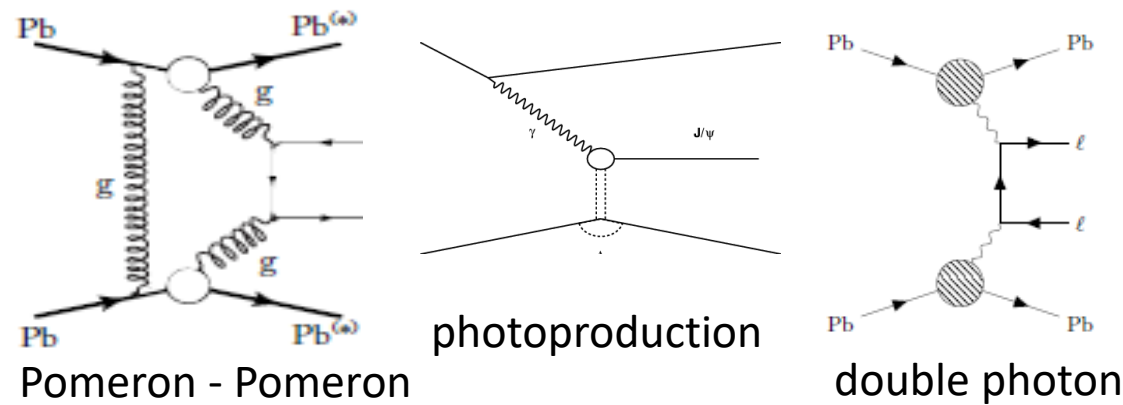
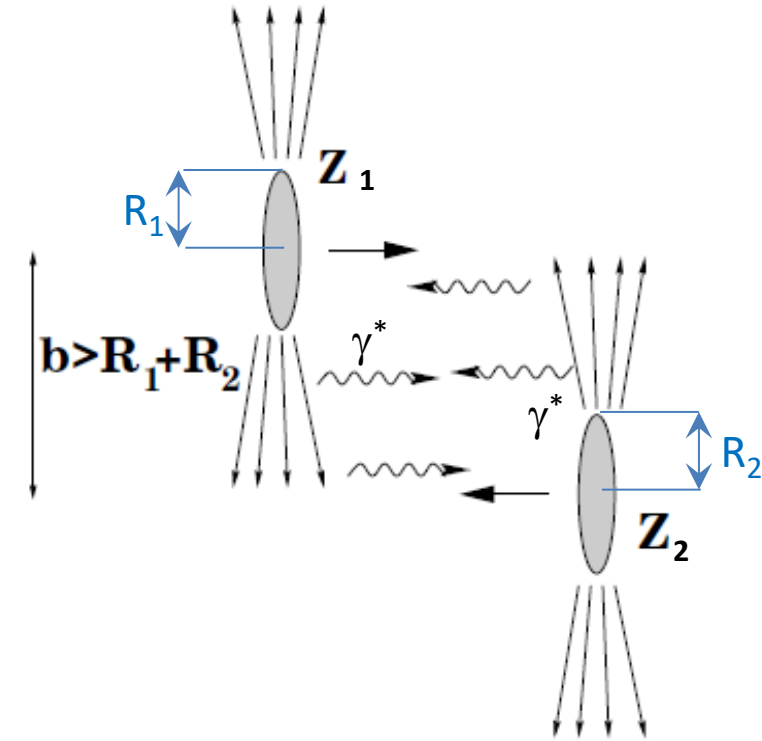
Outline

- Introduction
- Experimental apparatus
- Measurements
 - ρ^0 photoproduction in Pb-Pb and Xe-Xe
 - Excited ρ in two and four pion analysis in Pb-Pb
 - Coherent J/ψ photoproduction in Pb-Pb
 - Coherent $\psi(2S)$ photoproduction in Pb-Pb
- Summary



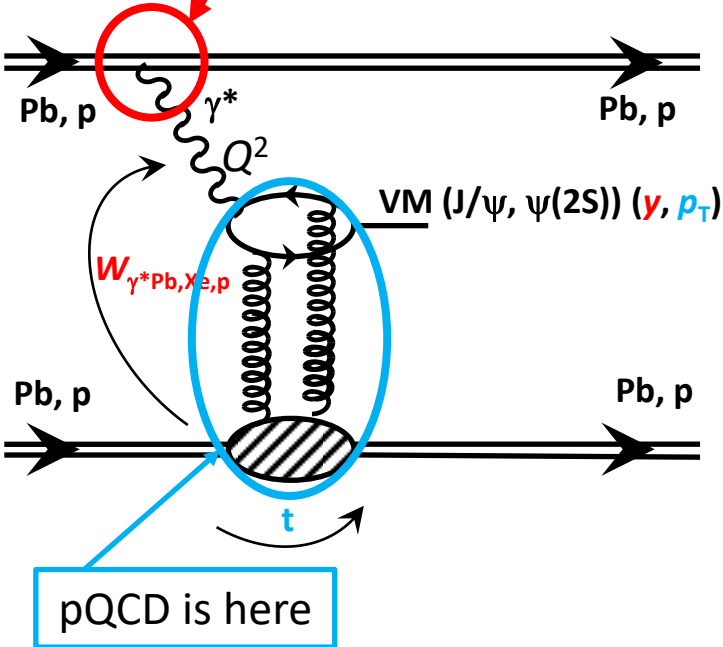
Ultra-peripheral collisions (UPC)

- Impact parameter $b > R_1 + R_2$
 - Hadronic interactions suppressed
- Photon induced reactions:
 - Well described in Weizsäcker-Williams approximation
 - Photon flux $\sim Z^2$ ($Z_{Pb} = 82$)
 - Large γ -induced interaction cross section
- Clear signature:
 - Low detector activity
 - Rapidity gap(s)
- Classes of processes:



Photoproduction and main variables

QED is here



pQCD is here

- Momentum scale $Q^2 \sim M_{VM}^2 / 4$
 - Hard scale assured by high mass of J/ψ , ψ' meson
 - Semi-hard scale for ρ^0 meson
- Vector Meson (VM) quantum numbers:
 - $J^{PC} = 1^{--}$
- Bjorken-x: fraction of longitudinal momentum of proton

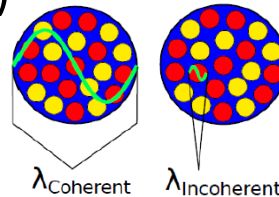
$$x_B = \frac{M_{VM}}{\sqrt{s_{NN}}} e^{\pm y}$$

- Photon-target centre-of-mass energy

$$W_{\gamma^* Pb,p}^2 = 2E_{Pb,p} M_{VM} e^{\mp y}$$
- 4-momentum transfer $|t| \sim p_T^2$

Coherent VM photoproduction:

- Photon couples coherently to all nucleons (whole nucleus)
- $\langle p_T^{VM} \rangle \sim 1/R_{Pb} \sim 50 \text{ MeV}/c$
- Target ion stays intact

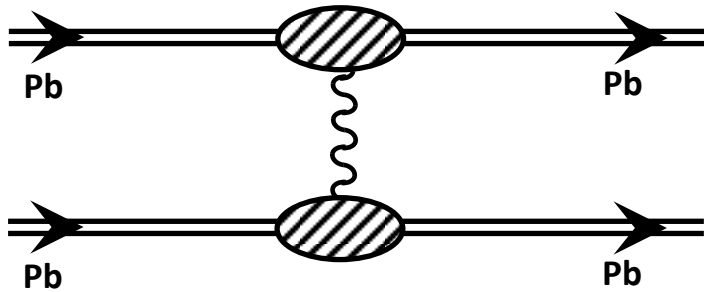


Incoherent VM photoproduction:

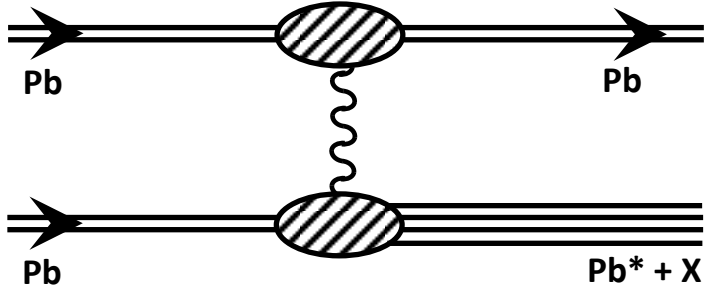
- Photon couples to a single nucleon
- $\langle p_T^{VM} \rangle \sim 1/R_p \sim 400 \text{ MeV}/c$
- Target ion breaks, nucleon stays intact
- Usually accompanied by neutron emission

Impact parameter dependence

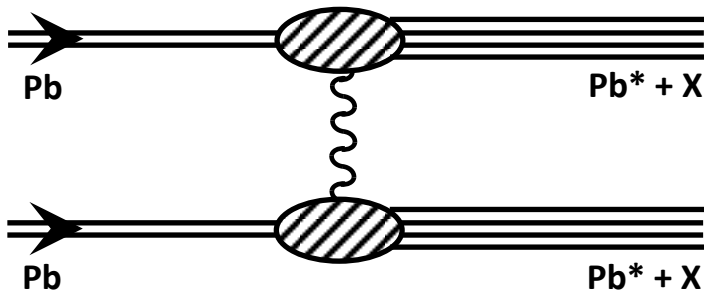
No breakup (0n0n)



Single breakup (Xn0n + 0nXn)



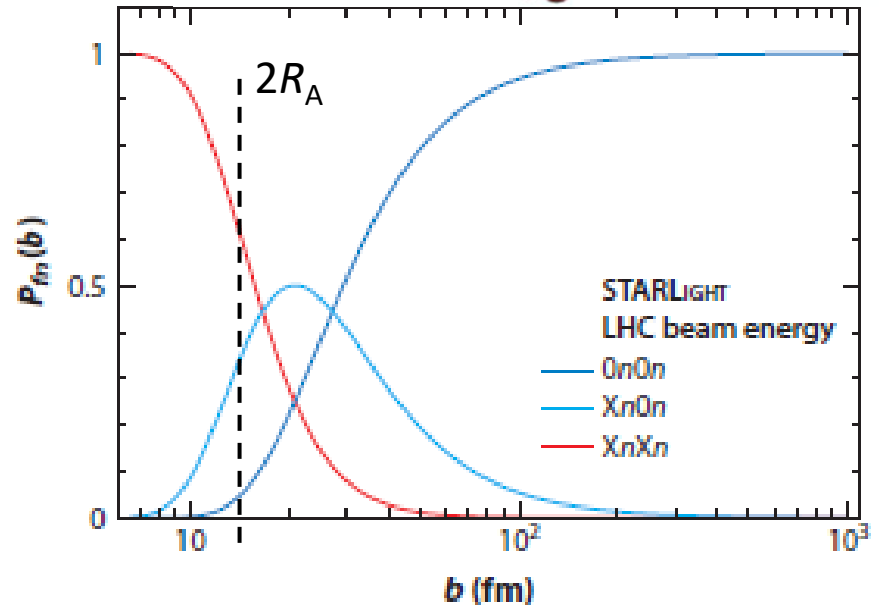
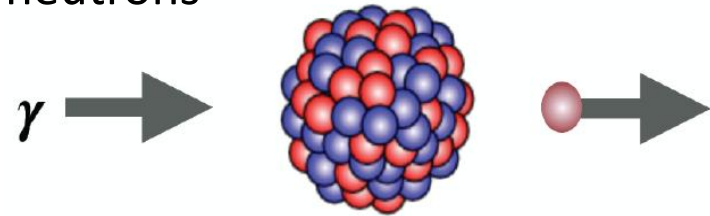
Double breakup (XnXn)



- Excitation of the nuclei possible through the secondary photon exchange

⇒ Giant dipole resonance

All protons vibrating against all neutrons →
Knocks out neutrons



UPC event classifier: 0n0n, 0nXn, XnXn
→ via electromagnetic dissociation (EMD)

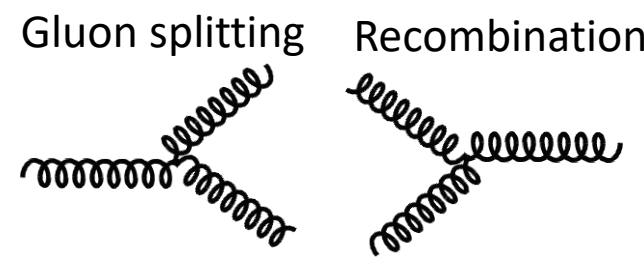
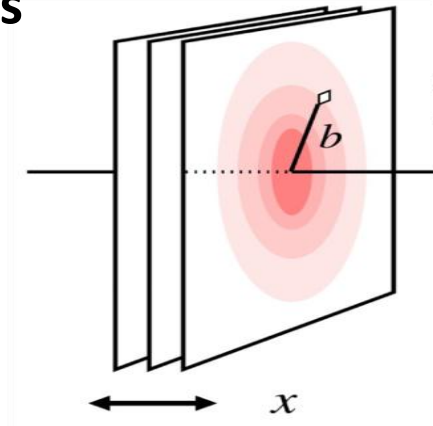
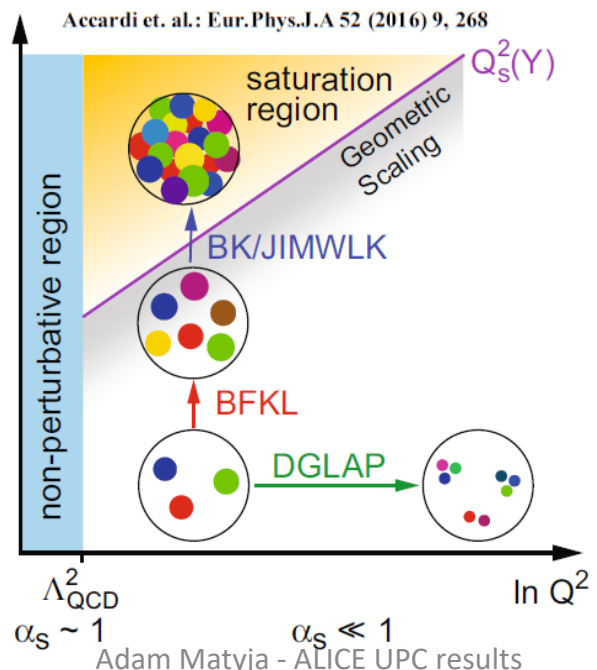
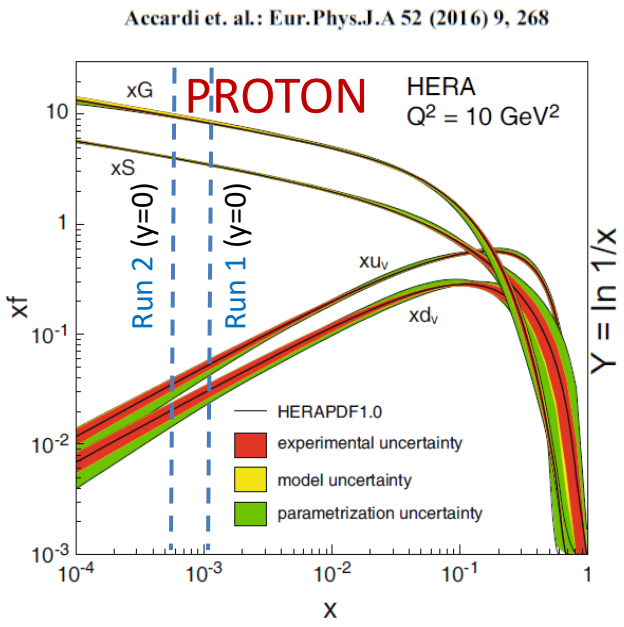
Motivation

- Coherent vector meson ($\rho^0, J/\psi$) photoproduction is sensitive to the **gluon density** evolution at low $x_B \rightarrow$ constrains **gluon shadowing**

$$\frac{d\sigma(\gamma p \rightarrow j/\psi p)}{dt} = |F^{2G}_N(t)|^2 \frac{\alpha_s^2 \Gamma_{ee}^J m^3 J \pi^3}{3\alpha_{em}} \left[xG(x, q^2) \frac{2q^2 |q_t J|^2}{(2q^2)^3} \right]^2$$

LO formula
Ryskin, Z. Phys. C 57, 89-92 (1993)

- $|t|$ -dependence helps to constrain **transverse gluonic** structure at low x_B and is sensitive to the gluon **saturation**
 - Saturation scale enhanced for nuclei by factor $A^{1/3}$: $(Q_s^A)^2 \approx cQ_0^2 [A/x]^{1/3}$
- Possibility of studies features of not well known **resonances**
- Constrain parameters of **models**



ALICE in Run 2

ALICE: *JINST* 3 S08002 (2008) ;
 Int. J. Mod. Phys. A29 (2014) 1430044

- a. ITS SPD Pixel
- b. ITS SDD Drift
- c. ITS SSD Strip
- d. V0 and T0
- e. FMD

ZDC

AD

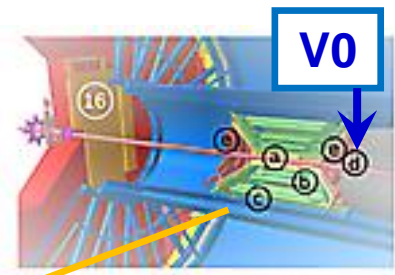
1. ITS
2. FMD, T0, V0
3. TPC
4. TRD
5. TOF
6. HMPID
7. EMCal
8. DCal
9. PHOS, CPV
10. L3 Magnet
11. Absorber
12. Muon Tracker
13. Muon Wall
14. Muon Trigger
15. Dipole Magnet
16. PMD
17. AD
18. ZDC
19. ACORDE

ITS

TPC

TOF

Muon Arm



- **Central Barrel tracking (e^\pm, h^\pm)**

- $|\eta| < 0.9, 0 < \varphi < 2\pi$
- ITS - silicon detector
- TPC - gas drift detector
- TOF - resistive plate chambers

- **Forward tracking (μ^\pm)**

- $-4 < \eta < -2.5$
- Absorber
- Muon tracker
- Muon trigger
- Dipole magnet

AD

ZDC

- **Diffractive detectors**

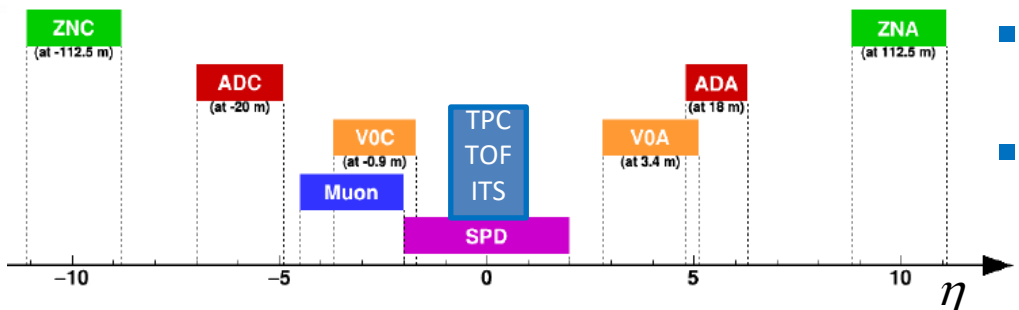
- AD - scintillator counter
- V0 - scintillator counter
- ZDC - sampling calorimeter

- **Vertex**

- Pixel

- **Trigger**

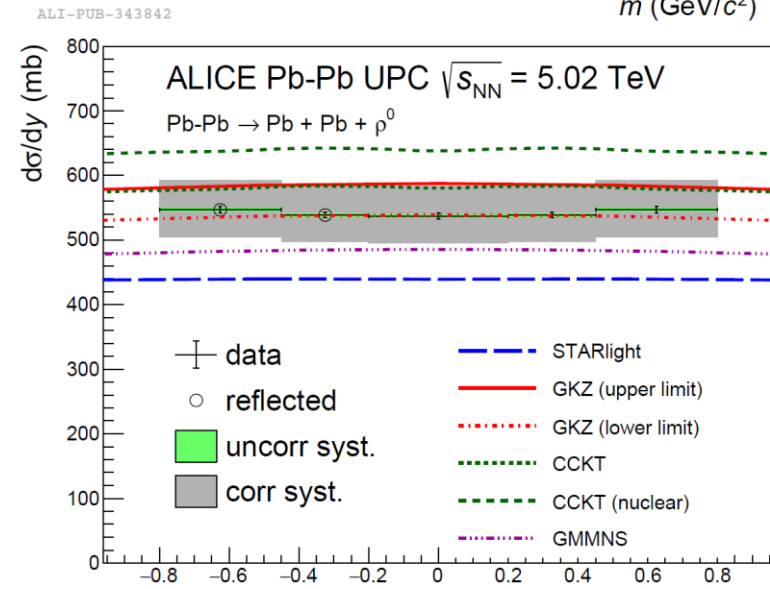
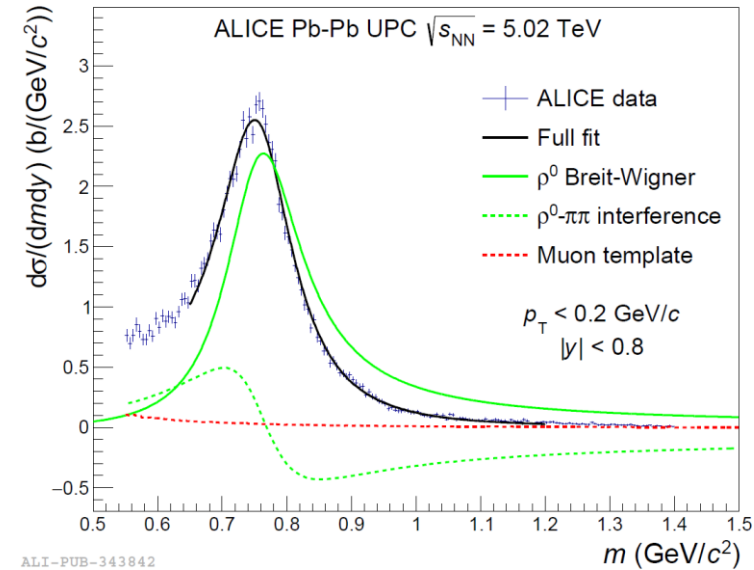
- SPD, TOF, AD, V0, Muon



ρ^0 in Pb-Pb at $\sqrt{s_{NN}} = 5.02$ TeV



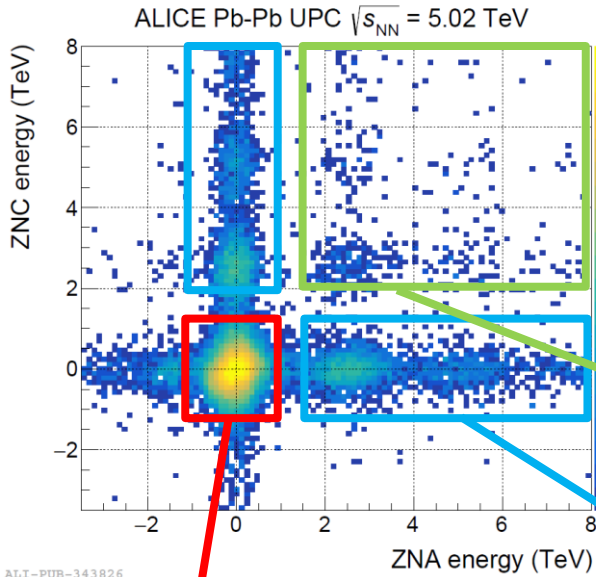
- Coherent $\rho^0 \rightarrow \pi^+ \pi^-$
 - $\frac{d\sigma}{dm dy} = |A \cdot BW_\rho + B|^2 + M$,
 - Pole mass and width agree with PDG
 - Large cross section (~ 550 mb) described by models
 - Measurement in nuclear breakup classes (0n0n, 0nXn, XnXn) to distinguish b dependence
- Comparisons with models
 - GKZ (nuclear shadowing) gives the best description
 - CCKT (saturation) is slightly worse
 - STARlight and GMMNS (saturation) underestimate



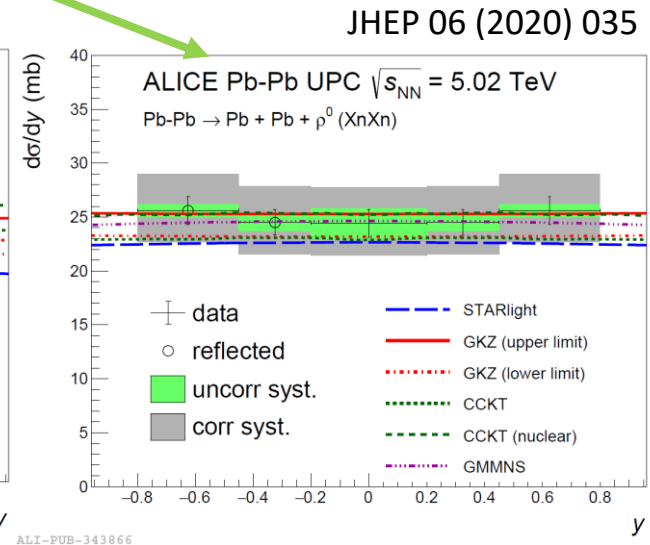
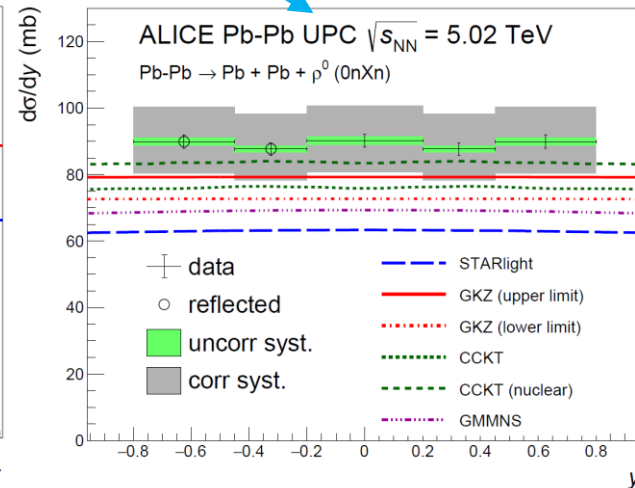
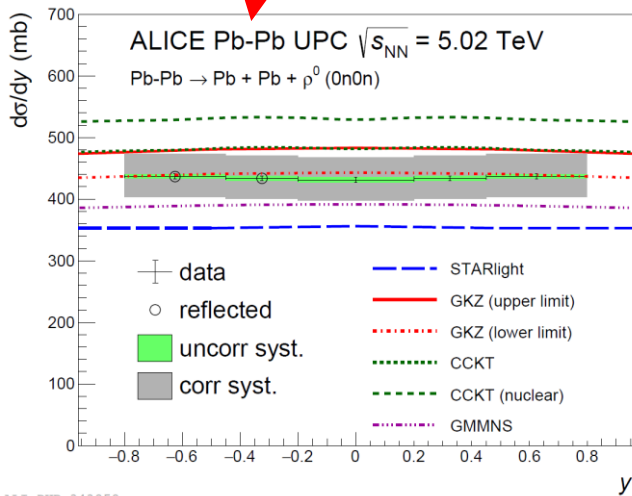
ALI-PUB-343854

ALICE, JHEP 06 (2020) 035

ρ^0 in Pb-Pb at $\sqrt{s_{NN}} = 5.02$ TeV



- Impact parameter dependence via ZDC selection in 3 classes: 0n0n, 0nXn, XnXn
- Comparisons with models
 - GKZ (nuclear shadowing) gives the best description
 - CCKT (saturation) is slightly worse
 - STARlight and GMMNS (saturation) underestimate
- Test of photon flux description



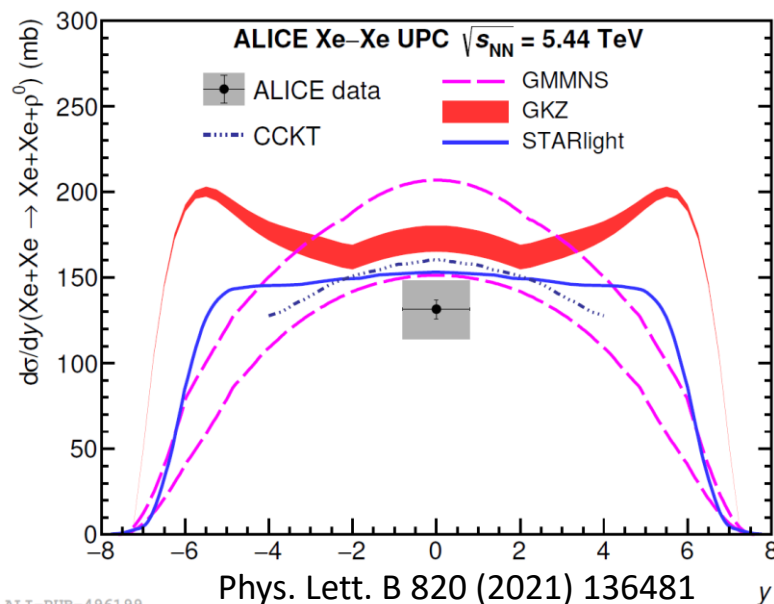
ρ^0 in Xe-Xe at $\sqrt{s_{NN}} = 5.44$ TeV



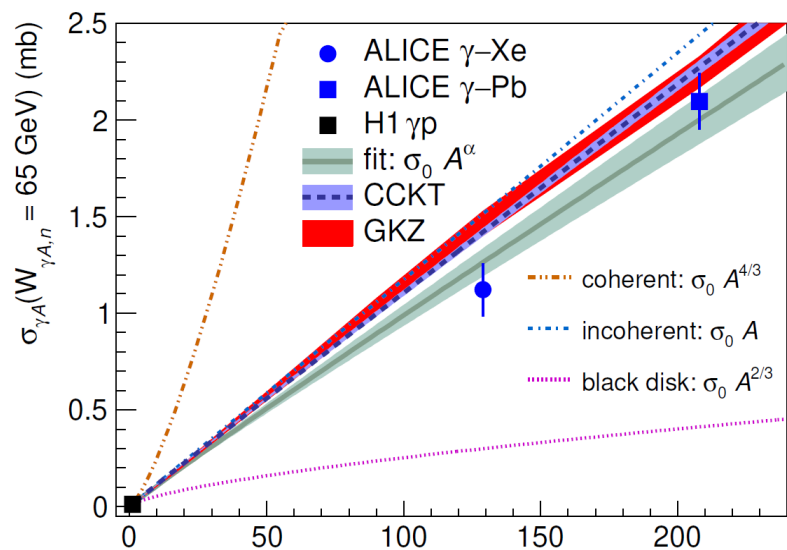
- $d\sigma/dy = 131.5 \pm 5.6^{\text{st}+17.5}_{-16.9}{}^{\text{sy}}$ mb
- All models relatively close to data

- $W_{\gamma A,n} = 65$ GeV
- $\sigma(\gamma A \rightarrow \rho^0 A) \sim A^\alpha$ with a slope $\alpha = 0.96 \pm 0.02^{\text{sy}}$
 - ⇒ Signals important **shadowing effect**
 - Far from black disk limit
 - Slope close to 1 by coincidence

- Fair description of data by models CCKT (saturation) and GKZ (shadowing)






ALI-PUB-496199

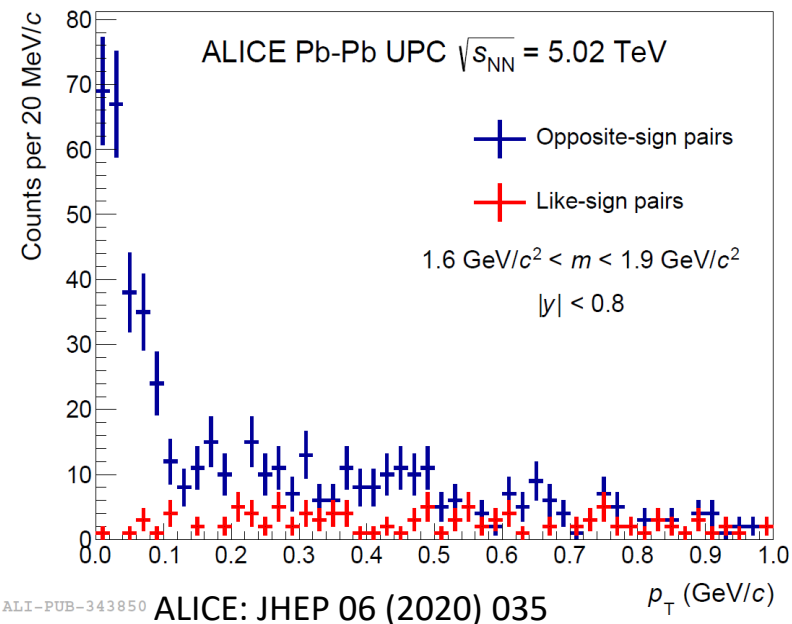
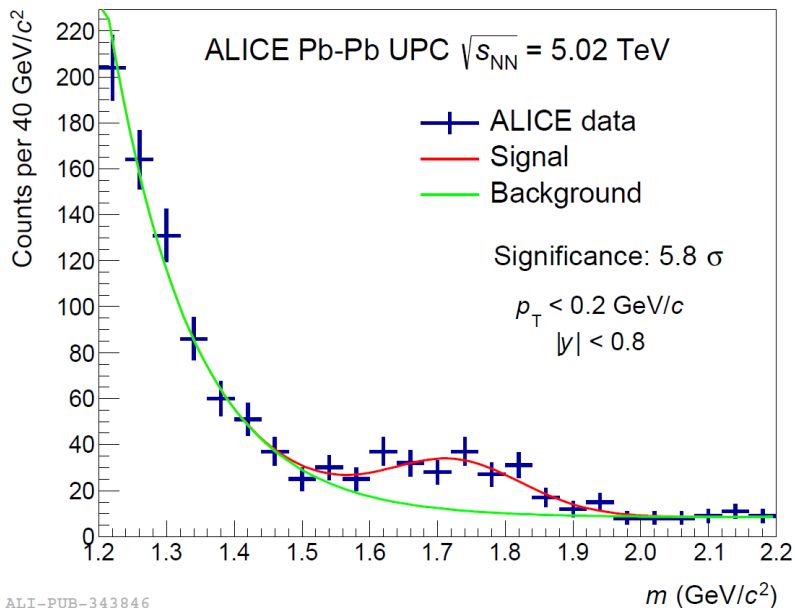


ALI-PUB-496203

Excited ρ in Pb-Pb at $\sqrt{s_{NN}} = 5.02$ TeV

- Resonance-like structure of two π at $M^{\pi\pi} \sim 1.7$ GeV/c²
 - Significance of 4.5σ
 - Seen also by STAR, ZEUS, H1   
 - Most probably $\rho_3(1690)$ with angular momentum $J = 3$
 - More data from Run3 + Run4 needed

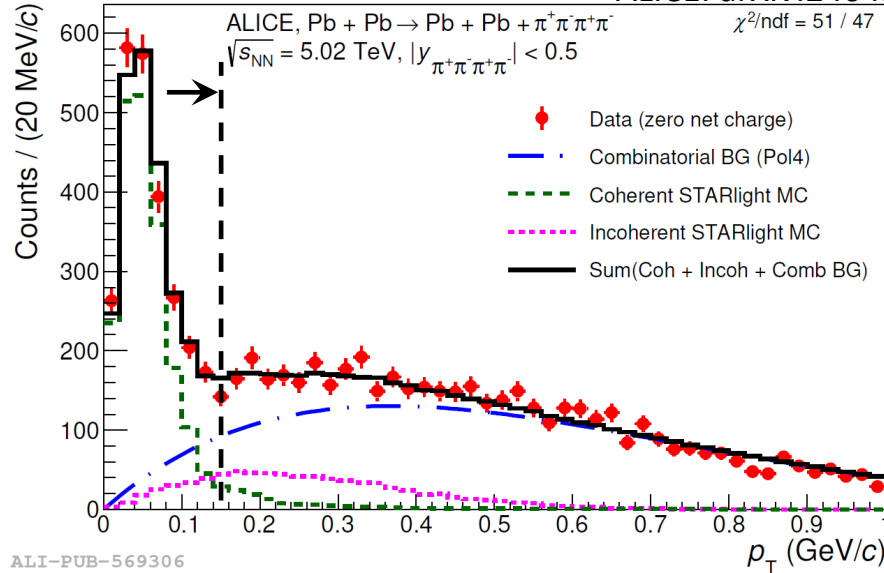
$$\frac{dN_{\pi\pi}}{dm} = P_1 \cdot \exp(-P_2 \cdot (m - 1.2 \text{ GeV}/c^2)) + P_3 + P_4 \cdot \exp(-(m - M_x)^2 / \Gamma_x^2)$$



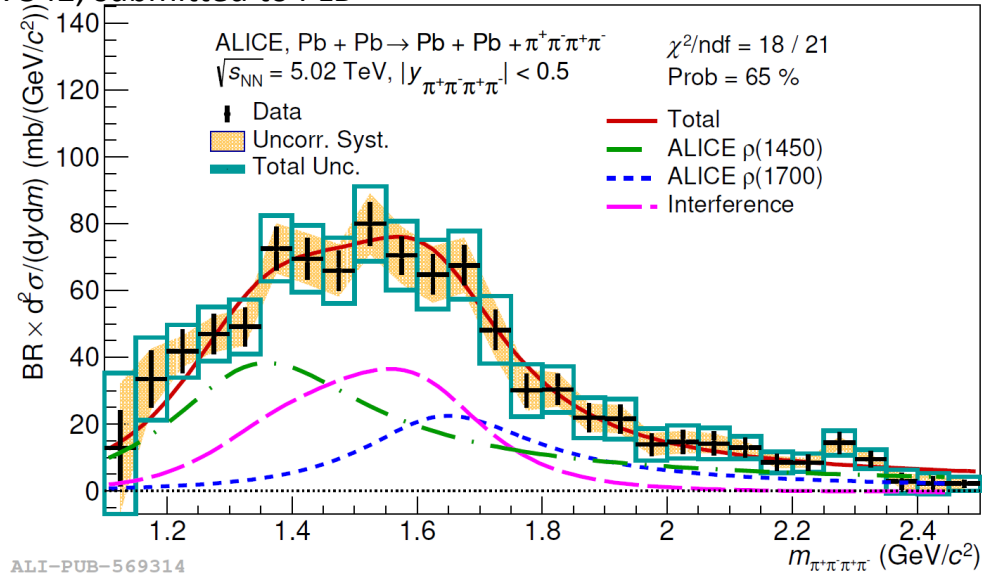
Exclusive four pion photoproduction



ALICE: arXiv:2404.07542, submitted to PLB



ALI-PUB-569306



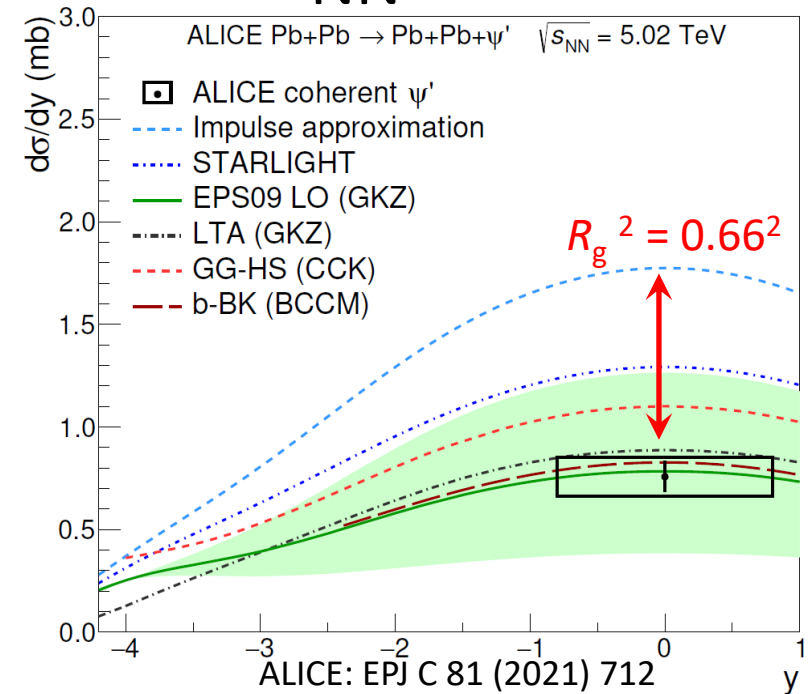
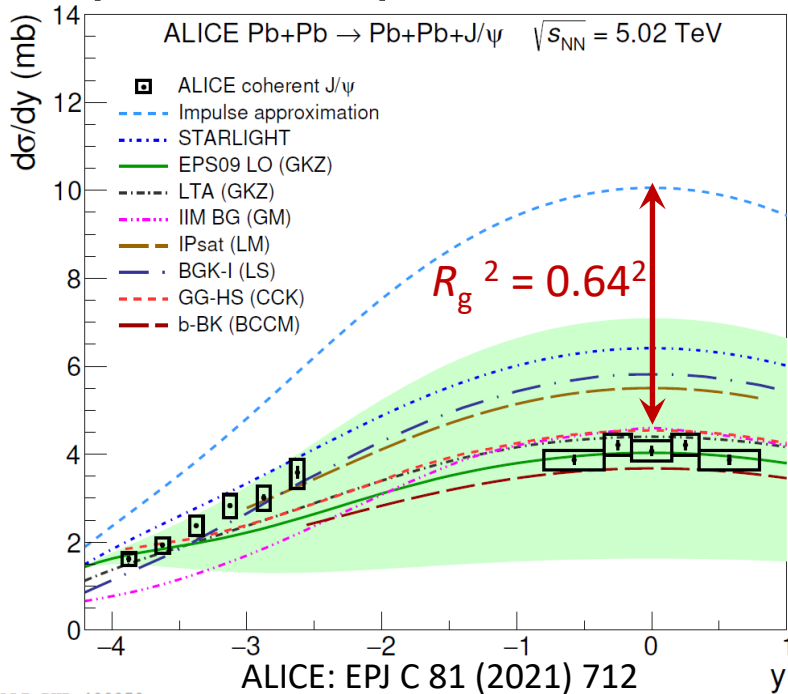
ALI-PUB-569314

- Excited ρ states expected
 - The mass and the width poorly measured
- $Pb\ Pb \rightarrow Pb\ Pb\ \pi^+\ \pi^-\ \pi^+\ \pi^-$
- Coherent component clearly seen
- Single resonance:
 - $\rho(1450)$: $47.8 \pm 2.3^{\text{stat}} \pm 7.7^{\text{syst}}$ mb
- Double resonance:
 - $\rho(1450)$: $24.8 \pm 2.5^{\text{stat}} \pm 8.1^{\text{syst}}$ mb
 - $\rho(1700)$: $10.1 \pm 2.3^{\text{stat}} \pm 5.3^{\text{syst}}$ mb

- Fully corrected invariant mass distribution fitted with a relativistic Breit-Wigner with a Söding term with one or two resonances
 - Single resonance fit in agreement with $\rho(1450)$ but disfavoured ($\chi^2/\text{ndf} = 48/25$)
 - Two resonances fit give better description ($\chi^2/\text{ndf} = 18/21$) and a rough agreement with PDG $\rho(1450)$ and $\rho(1700)$ with mixing angle

$$\frac{d\sigma}{dm_{\pi\pi\pi\pi}} = \left| A \cdot BW_1 + e^{-i\phi} B \cdot BW_2 \right|^2$$

J/ψ and ψ(2S) in Pb-Pb at $\sqrt{s_{NN}} = 5$ TeV



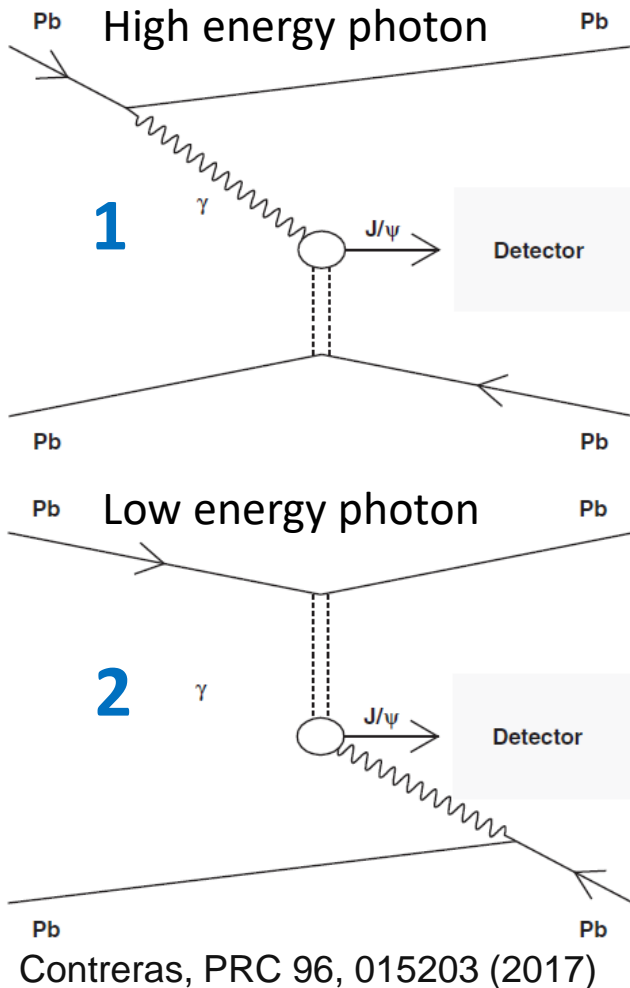
- **Wide rapidity range:** Forward (J/ψ) and Central (both) region
- **Nuclear gluon shadowing factor** for $0.3 \times 10^{-3} < x_B < 1.4 \times 10^{-3}$
 - $R_g = 0.64 \pm 0.04$ for J/ψ
 - $R_g = 0.66 \pm 0.06$ for ψ(2S)
- **No model describes the full rapidity dependence**
 - Models with nuclear shadowing (EPS09 LO, LTA) or saturation (GG-HS for J/ψ, b-BK for ψ(2S)) describe central and very forward data but **tensions** in semiforward region
 - Other models describe either (semi-)forward or central rapidity region

Rapidity dependance: Ambiguity problem

ALICE: EPJ C 81 (2021) 712

- Two sources \Rightarrow two values of x_B

$$\frac{d\sigma_{AA \rightarrow AA' J/\psi}}{dy} = N(\omega_{\gamma 1}) \sigma_{\gamma A}(\omega_{\gamma 1}) + N(\omega_{\gamma 2}) \sigma_{\gamma A}(\omega_{\gamma 2})$$



Photon flux

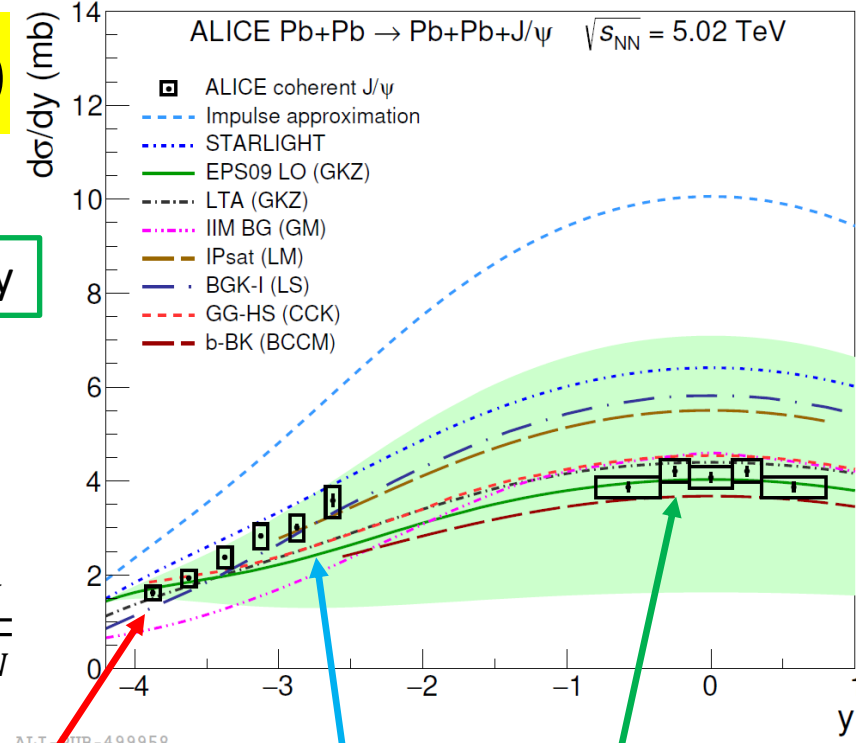
Photon energy

$$\omega_{\gamma 1} = \frac{M_{VM}}{2} e^{+y}$$

$$x_B = \frac{1}{\omega_{\gamma 1, \gamma 2}} \frac{M_{VM}^2}{2\sqrt{s_{NN}}}$$

1: 5 % $x_B \sim 1.1 \times 10^{-5}$
 2: 95 % $x_B \sim 3.3 \times 10^{-2}$

$$\omega_{\gamma 2} = \frac{M_{VM}}{2} e^{-y}$$



50 % each $x_B \sim 10^{-3}$

1: 40 % $x_B \sim 5.1 \times 10^{-4}$
 2: 60 % $x_B \sim 0.7 \times 10^{-2}$

Solving the ambiguity problem

$$\frac{d\sigma_{AA \rightarrow AA' J/\psi}}{dy} = N(\omega_{\gamma 1})\sigma_{\gamma A}(\omega_{\gamma 1}) + N(\omega_{\gamma 2})\sigma_{\gamma A}(\omega_{\gamma 2})$$

Coherent J/ψ at **midrapidity**

- UPC cross section can be directly linked to photonuclear cross section

$$\frac{d\sigma}{dy} = 2N(\omega_{\gamma})\sigma_{\gamma Pb}(\omega_{\gamma})$$

Coherent J/ψ at **forward rapidity**

- 95% of the cross section comes from the low energy photon (high x_B gluon)

$$\frac{d\sigma}{dy} \cong N(\omega_{\gamma 2})\sigma_{\gamma Pb}(\omega_{\gamma 2})$$

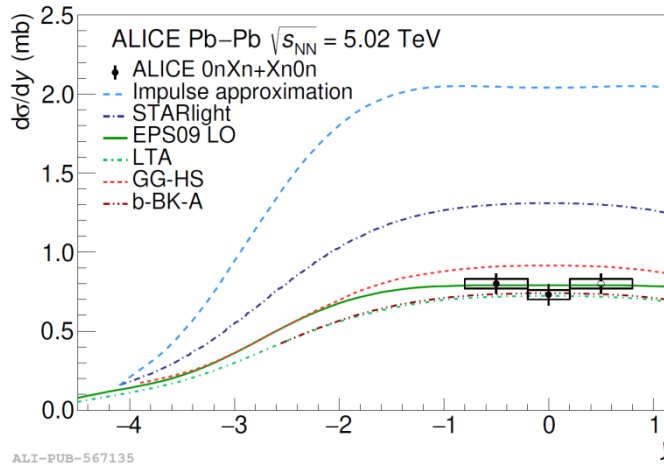
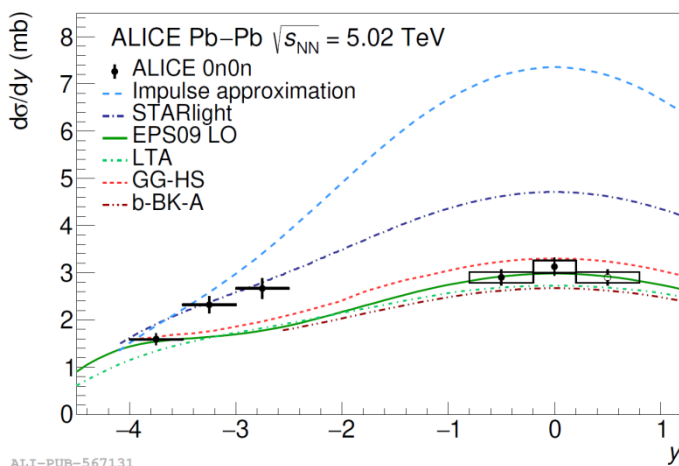
To disentangle both photon contributions we need to measure the same process in **peripheral** collisions or with **EMD**!

$$\frac{d\sigma_{PbPb}}{dy} = \frac{d\sigma_{PbPb}^{0N0N}}{dy} + 2\frac{d\sigma_{PbPb}^{0NXN}}{dy} + \frac{d\sigma_{PbPb}^{XNXN}}{dy}$$

Guzey et al., EPJC 74 (2014) 7, 2942

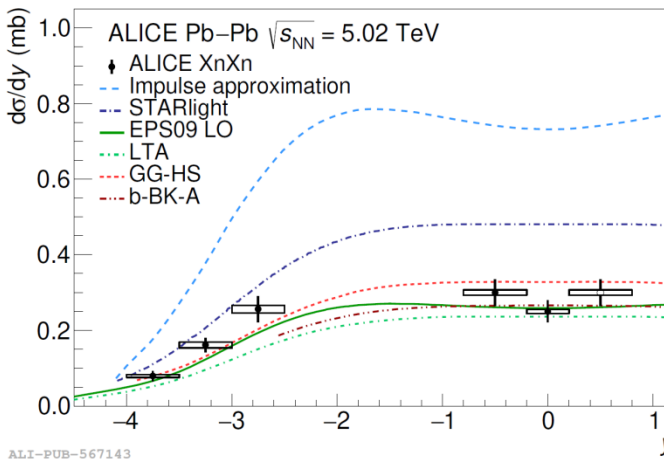
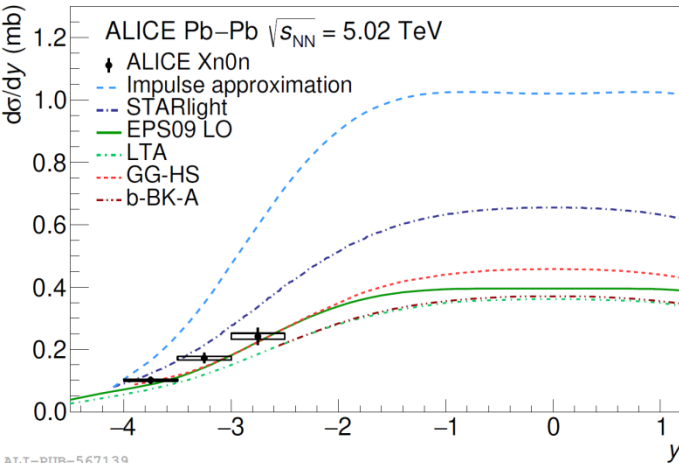
$\frac{d\sigma_{PbPb}^{0N0N}}{dy}$	=	$N^{0N0N}(\omega_{\gamma 1}, +y)\sigma_{\gamma Pb}(\omega_{\gamma 1}, +y)$	+	$N^{0N0N}(\omega_{\gamma 2}, -y)\sigma_{\gamma Pb}(\omega_{\gamma 2}, -y)$	
$\frac{d\sigma_{PbPb}^{0NXN}}{dy}$	=	$N^{0NXN}(\omega_{\gamma 1}, +y)\sigma_{\gamma Pb}(\omega_{\gamma 1}, +y)$	+	$N^{0NXN}(\omega_{\gamma 2}, -y)\sigma_{\gamma Pb}(\omega_{\gamma 2}, -y)$	
measured		theory		extracted	

Coherent J/ψ in neutron classes



ALI-PUB-567131

ALI-PUB-567135



ALI-PUB-567139

ALI-PUB-567143

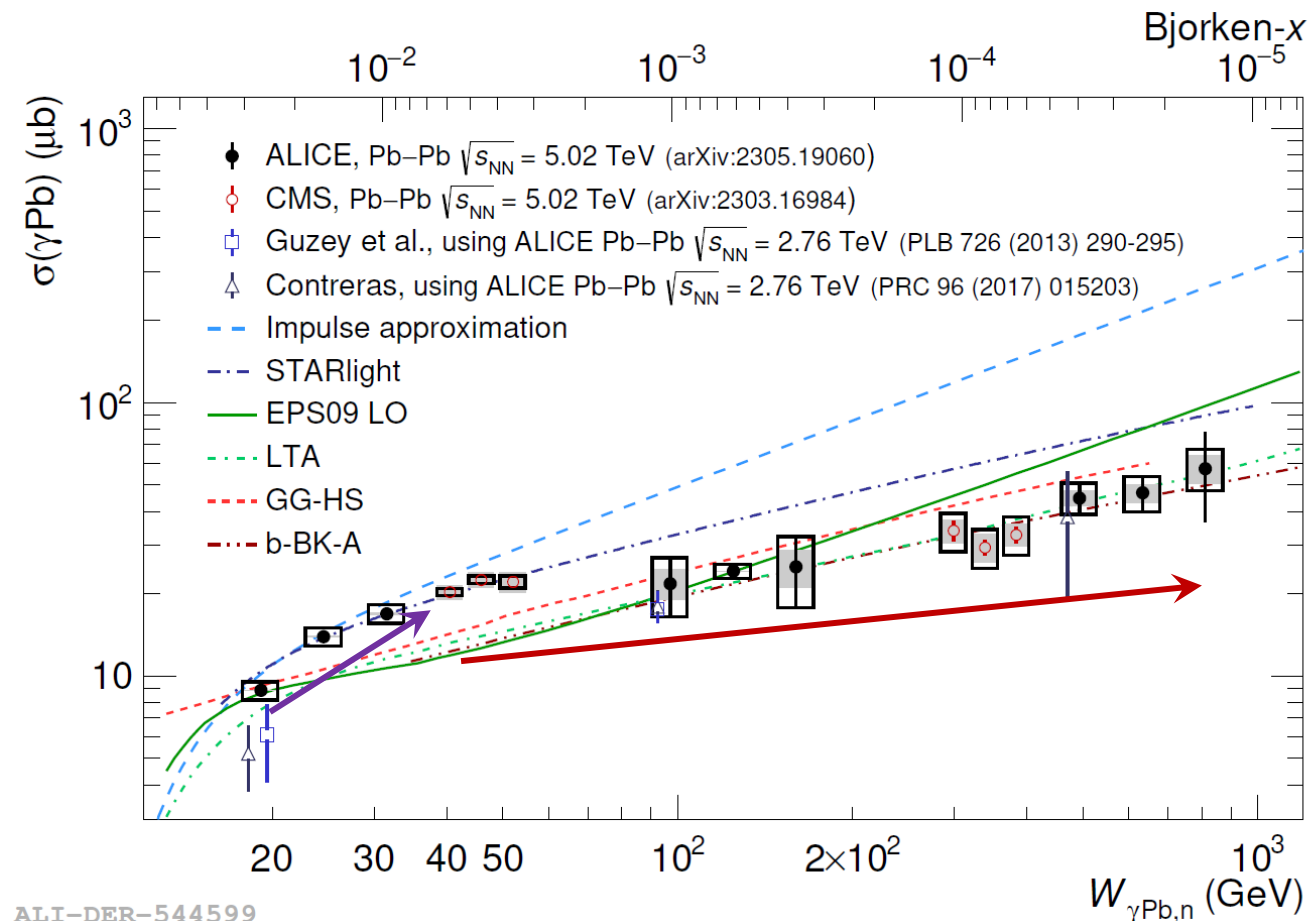
Corrected for:

- Event migration among classes
- Neutrons from pile-up
- Charged particle production from dissociation of either nuclei

ALICE: *JHEP* 10 (2023) 119

- 0n0n class has the largest statistics, XnXn – the lowest one
- Sensitivity to test theoretical models
- Good test of photon fluxes

Energy dependence of coherent J/ψ

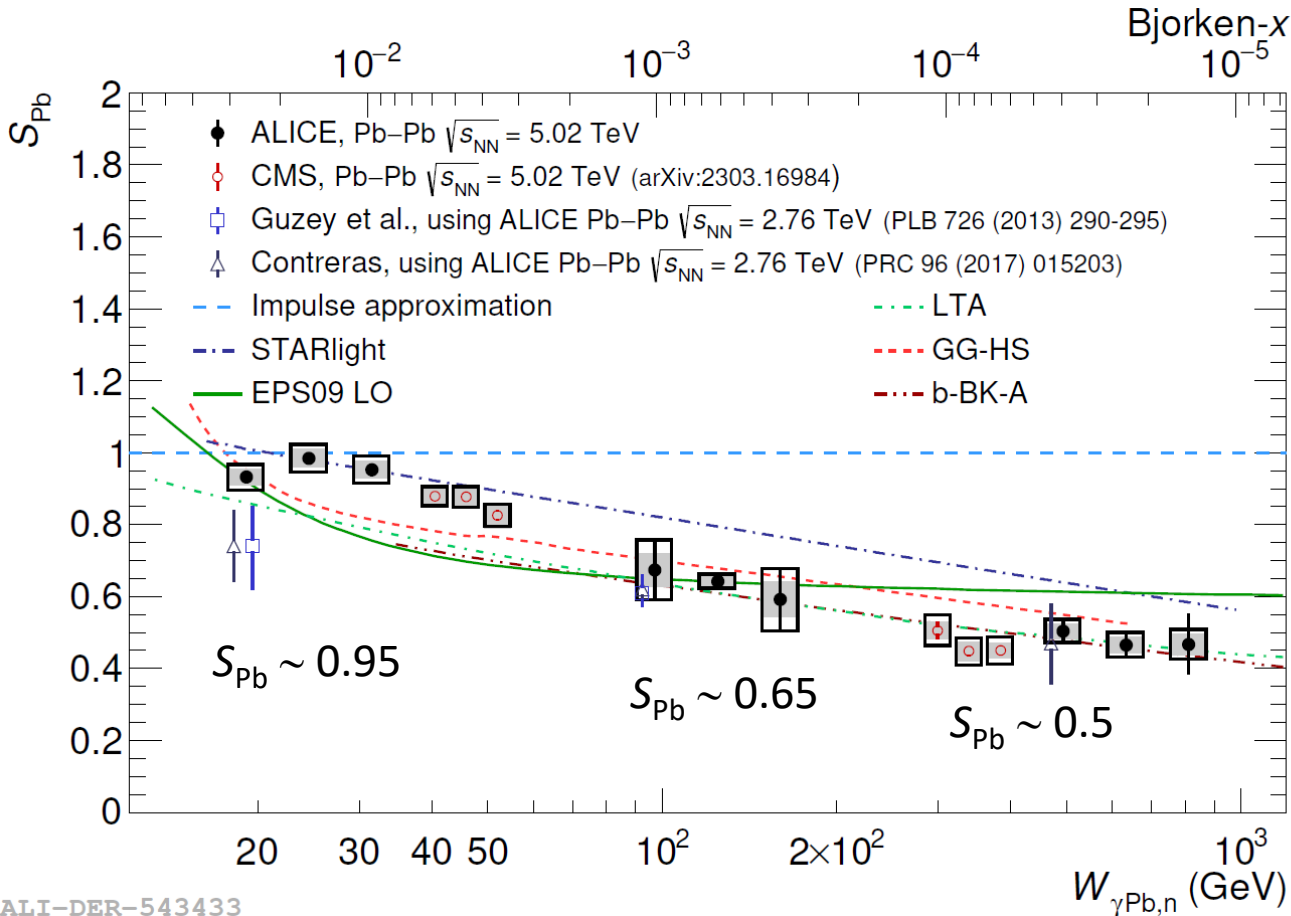


- First measurement of the energy dependence of the photonuclear cross section down to $x_B \sim 10^{-5}$
- Or very wide energy range (20 - 800 GeV)
- Consistency between two methods: Run 1 with peripheral collisions and Run 2 data with neutron emission classes
- Similar trend for the energy dependence observed in both CMS and ALICE
- Both saturation and shadowing models are favored at low- x_B

ALICE: JHEP 10 (2023) 119

- Rise at low $W_{\gamma\text{Pb},n} \sim 15$ GeV $\rightarrow \sim 40$ GeV
 \Rightarrow consistent with fast-growing gluon densities toward lower x_B
- Flattish trend from $W_{\gamma\text{N}} \sim 40$ GeV $\rightarrow \sim 800$ GeV

Nuclear suppression factor of coh. J/ψ



- First measurement of the nuclear suppression factor down to $x_B \sim 1.1 \times 10^{-5}$
- Additional uncertainty from impulse approximation
- Low energy (high x_B):
 - Impulse approximation
 - STARlight
 - $S_{Pb} \sim 0.95$
- High energy (low x_B):
 - data favours both saturation (b-BK-A, GG-HS) and shadowing (LTA) models
 - $S_{Pb} \sim 0.5$

ALICE: JHEP 10 (2023) 119

No model describes the whole energy/Bjorken-x range!

$$S_{Pb} = \sqrt{\frac{\sigma_{\gamma Pb}}{\sigma_{\gamma Pb}^{IA}}}$$

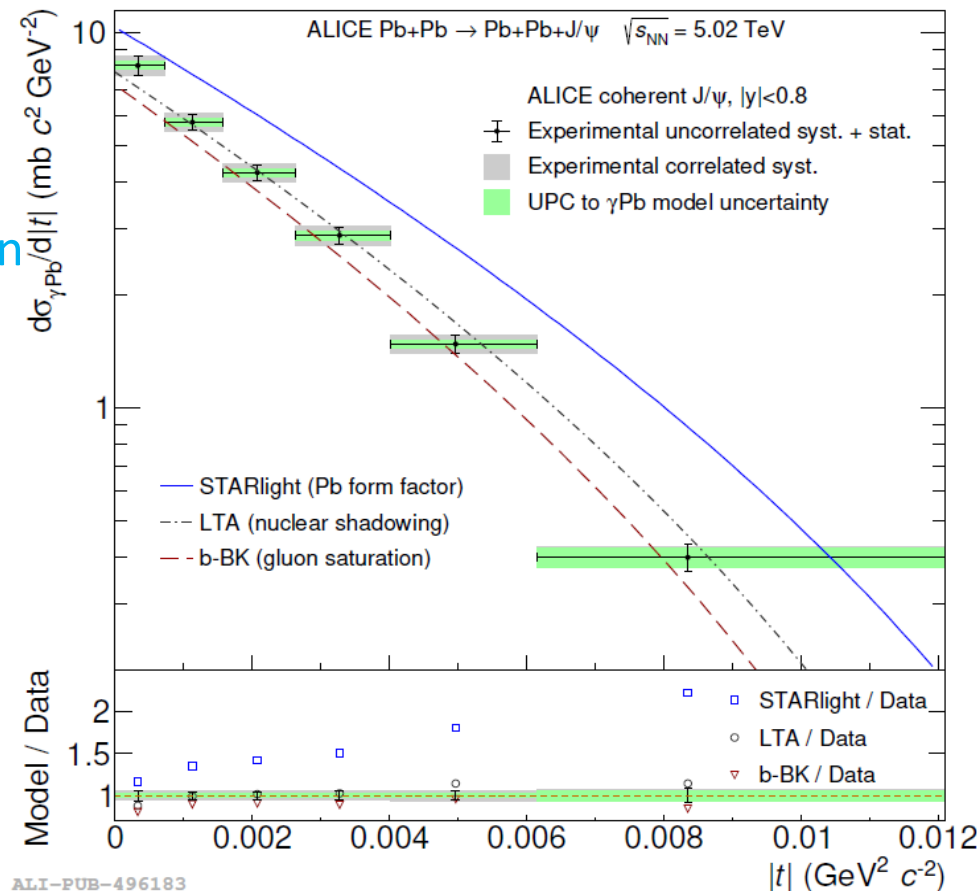
Coherent J/ψ

ALICE: PLB 817 (2021) 136280

- Gluon density is impact parameter b dependent at given Bjorken- x and Q^2
- b and p_T are Fourier conjugates
- $p_T^2 \approx |t|$ dependence of coherent J/ψ photoproduction is sensitive to the gluon distribution in the transverse plane
- HERA-like precision achieved
- Bayesian and SVD unfolding used to transform $p_T^2 \rightarrow |t|$
- Transition from UPC to photonuclear cross section

$$\left. \frac{d^2 \sigma_{J/\psi}^{coh}}{dy dp_T^2} \right|_{y=0} = 2n_{\gamma Pb}(y=0) \frac{d\sigma_{\gamma Pb}}{d|t|}$$

- Comparison to models:
 - STARlight does not have shadowing, so does not describe shape nor magnitude
 - LTA contains nuclear shadowing – agrees with data
 - b-BK based on gluon saturation – agrees with data



ALI-PUB-496183

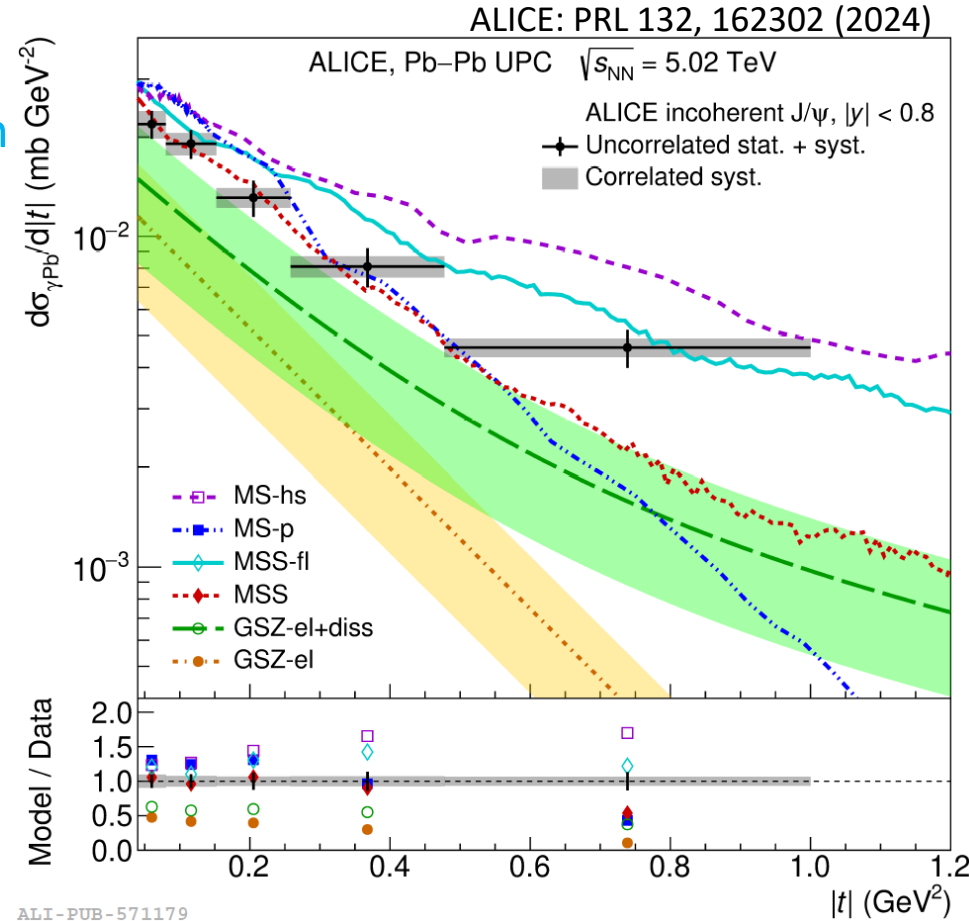
- LTA** (shadowing): PRC 95 (2) (2017) 025204;
 - vector dominance model (VDM) based on perturbative Leading Twist Approximation (LTA) of nuclear shadowing.
- b-BK** (saturation): arXiv:2006.12980 [hep-ph];
 - impact parameter dependent BK computation.

Incoherent J/ψ

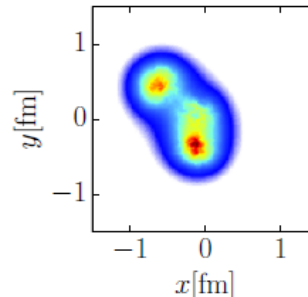
- **$|t|$ dependence** of the **incoherent J/ψ** photoproduction is sensitive to the **variance of the spatial gluon distribution** in the transverse plane (**quantum fluctuations**)

$$\frac{d\sigma^{inc}}{dt} = \frac{Rg^2}{16\pi} (\langle |A(x, Q^2, \vec{\Delta})|^2 \rangle - |\langle A(x, Q^2, \vec{\Delta}) \rangle|^2)$$

- This measurement probes **fluctuations** of the gluonic „hot spots” in Pb
- Larger $|t|$ range \rightarrow scatter of smaller object
- Models fail to predict the normalisation
- Normalization is linked to the scaling from proton to nuclear targets
- (Slope of) **data favor models with gluonic subnucleon fluctuations** (hot spots in **MS-hs**, fluctuations **MSS-fl** and dissociation in **GSZ el+dis**)



ALI-PUB-571179



- MS** (saturation): PLB 772 (2017) 832;
- Based on IPsat model.
- GSZ** (shadowing): PRC 99 (2019) 015201;
- VDM based on LTA shadowing including elastic and/or dissociative part
- MSS** (saturation): PRD 106, 7 (2022) 074019
- Based on JIMWLK equations.

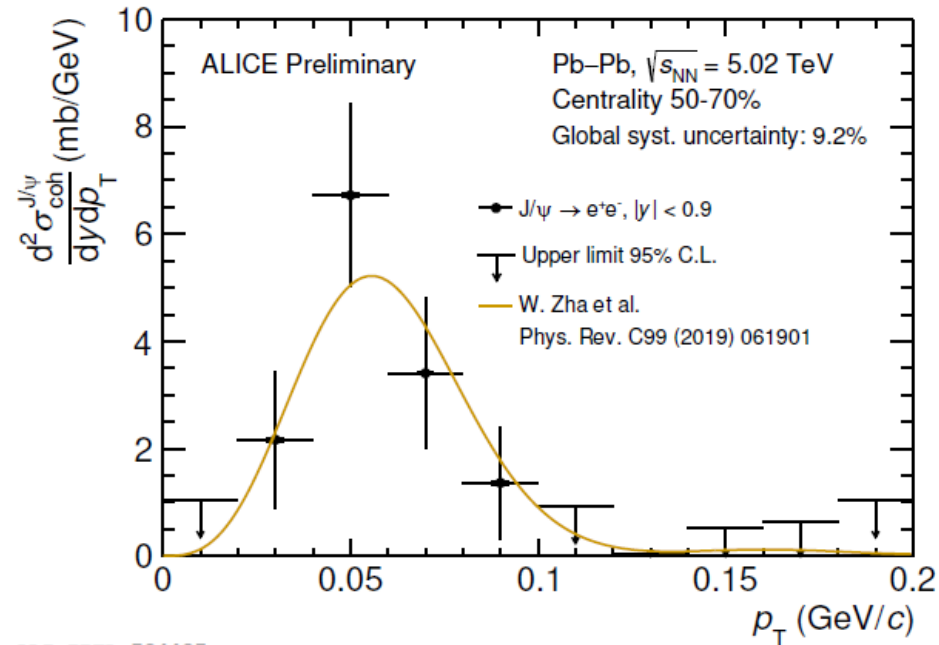
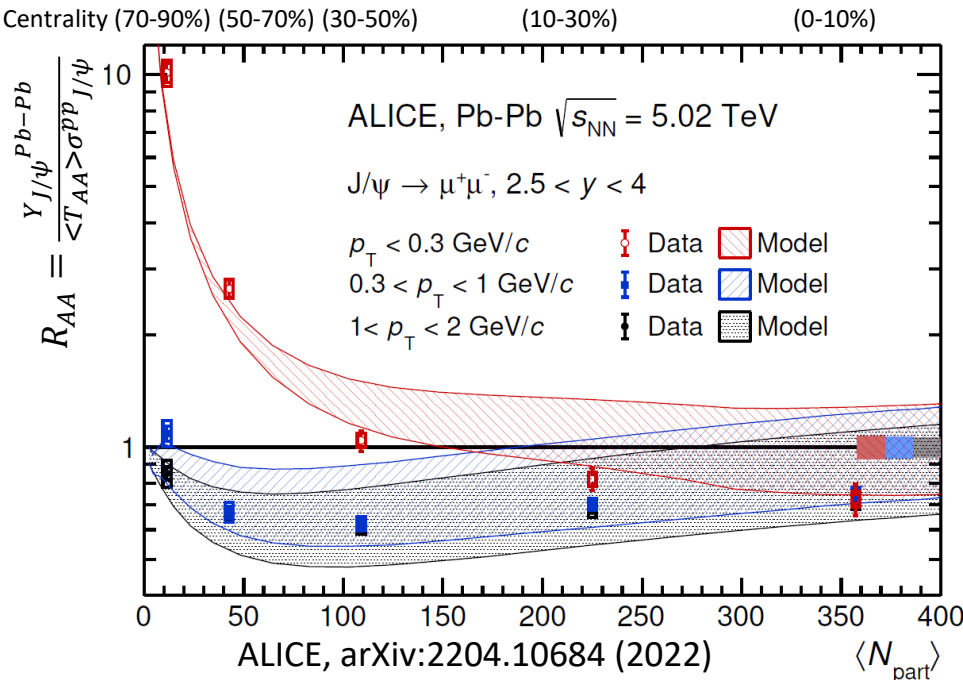
Summary

- ρ^0 photoproduction signals large shadowing effects (Pb-Pb, Xe-Xe)
- New excited ρ states visible, but more precise data needed
- Nuclear gluon structure probed with J/ψ and $\psi(2S)$ at $x_B \sim 10^{-3} - 10^{-5}$
 - Nuclear gluon shadowing factor $R_g \sim 0.65$ at $x_B \sim 10^{-3}$
 - Models with shadowing or saturation describe data the best
 - No model currently describe the rapidity dependence
 - $|t|$ dependence shows importance of subnucleon fluctuations
- Awaiting new results from Run 3

Backup

J/ψ photoproduction in non UPC Pb-Pb

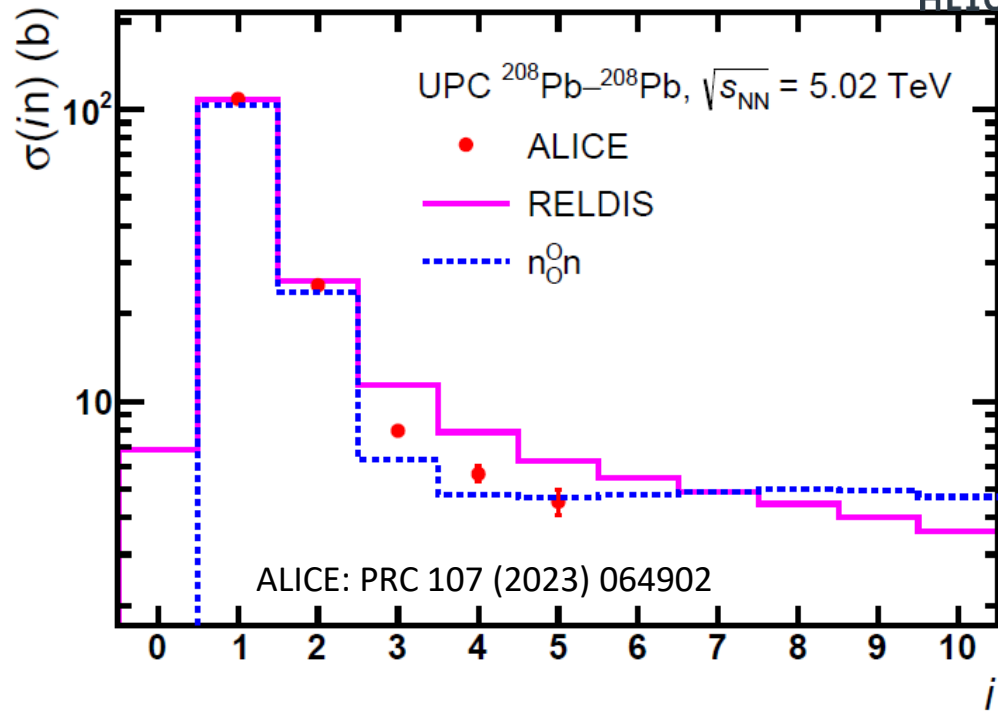
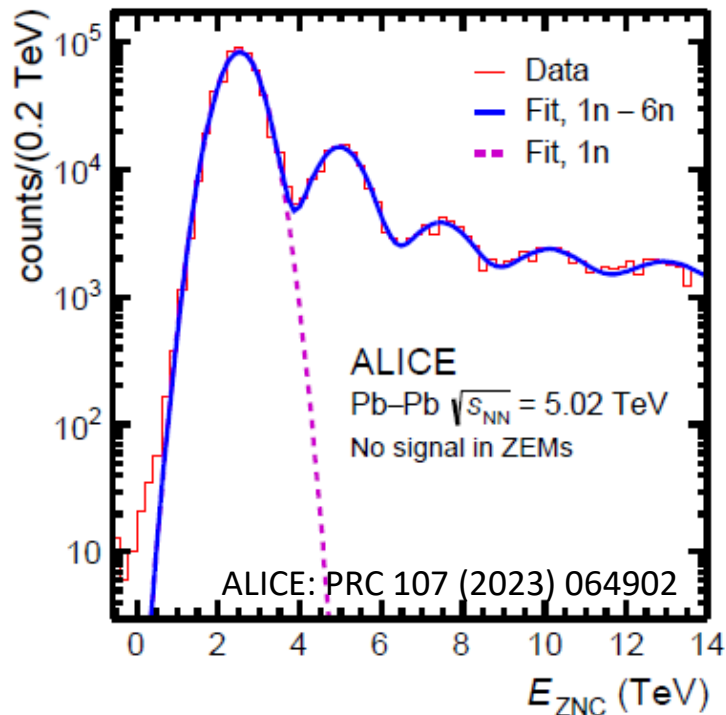
- **Low p_T (< 0.3 GeV/c) and R_{AA} excess** explained by photoproduction in **peripheral** collisions
- Hadroproduction dominates in higher p_T intervals
- Good description of R_{AA} by model (W. Shi et al.) with medium effects + photoproduction. QGP effects also considered
- Both **forward** and **central** region



Neutron emission in UPC



ALICE



ZN	$\sigma(in)$ (b)	$\sigma^{RELDIS}(in)$ (b)	$\sigma^{n_0^n}(in)$ (b)
1n	$108.4 \pm 0.1 \pm 3.7$	108.0 ± 5.4	103.7 ± 2.1
2n	$25.0 \pm 0.1 \pm 1.3$	25.9 ± 1.3	23.6 ± 0.5
3n	$7.95 \pm 0.04 \pm 0.23$	11.4 ± 0.6	6.3 ± 0.1
4n	$5.65 \pm 0.03 \pm 0.33$	7.8 ± 0.4	4.8 ± 0.1
5n	$4.54 \pm 0.03 \pm 0.44$	6.3 ± 0.3	4.7 ± 0.1
1n-5n	$151.5 \pm 0.2 \pm 4.6$	159.8 ± 5.6	143.1 ± 2.2

ALICE: PRC 107 (2023) 064902

- It is huge!
- Up to 5 neutrons
- Hadronic cross section $\sigma_{had} = 7.67 \pm 0.24$ b
- Good description of 1n and 2n emission, but other classes are not so well described

RELDIS: Phys. Part. Nucl. 42 (2011) 215.

NOON: Comput. Phys. Commun. 253 (2020) 107181.

Photonuclear J/ψ cross section



ALICE

- Gluon distribution at **HERA** energies follows power law at low x_B
 \Rightarrow similar trend in $W_{\gamma p}$
- **Exclusive J/ψ cross section** at LHC follows HERA trend so far

ALICE: p-Pb at $\sqrt{s_{NN}} = 5.02$ and 8.16 TeV

LHCb: pp at $\sqrt{s} = 7$ and 13 TeV

- Power law fit $\sigma \sim W_{\gamma p}^\delta$

H1 data: $\delta = 0.67 \pm 0.03$

ALICE data: $\delta = 0.7 \pm 0.04$

\Rightarrow agreement LHC and **HERA**

\Rightarrow agreement **ALICE** and **LHCb**

- Models show agreement

- JMRT NLO: based on DGLAP evolution with dominant NLO contribution

- valid to $x_B \sim 2 \times 10^{-5}$

- CCT: Saturation in an energy dependent hot spot model

- Probe wide region $x_B \sim 10^{-2} - 10^{-6}$

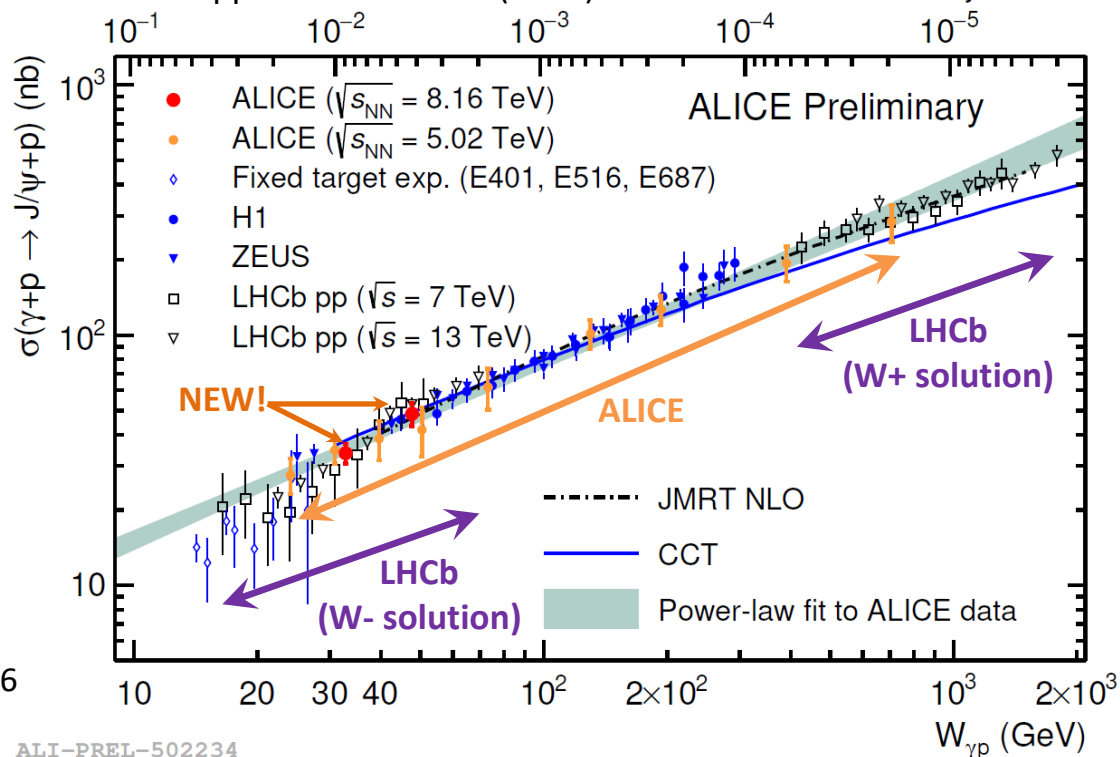
ALICE p-Pb 8.16 TeV: NEW

ALICE p-Pb 5.02 TeV: Phys. Rev. Lett. 113 (2014) 232504.

LHCb pp 7 TeV: J. Phys. G: Nucl. Part. Phys. 41 (2014) 055002;

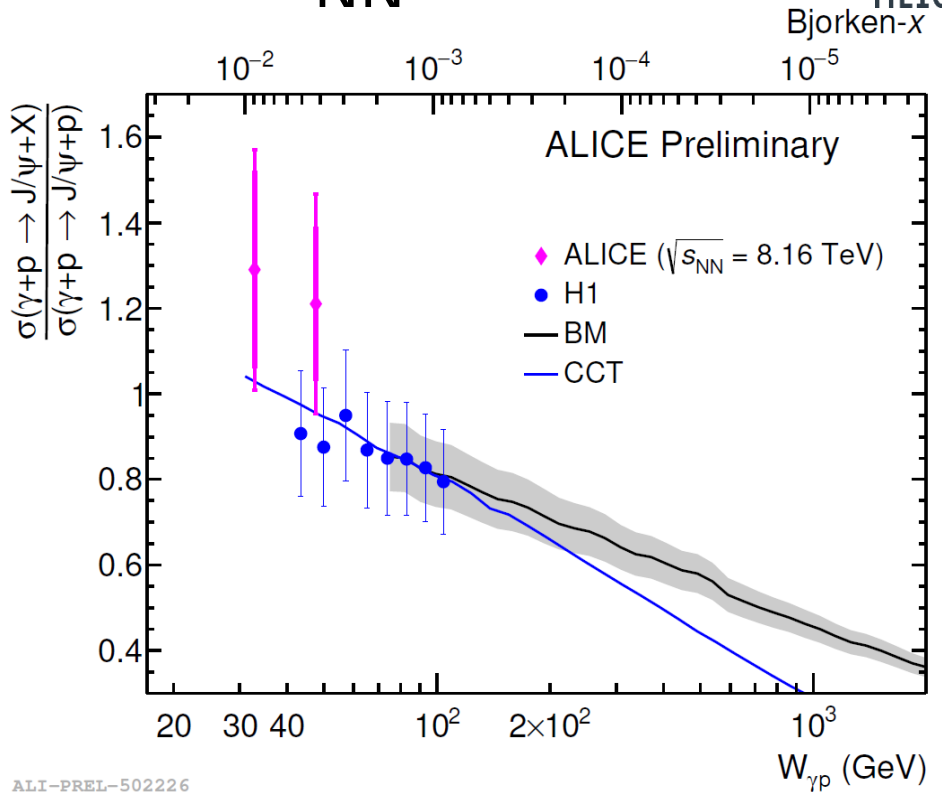
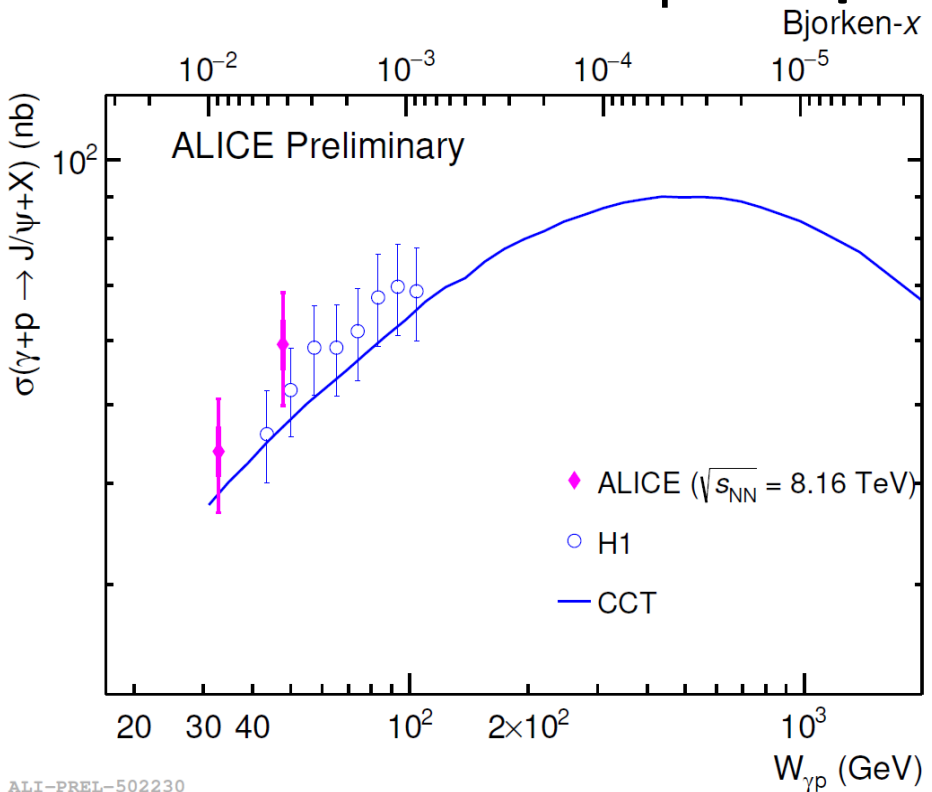
LHCb pp 13 TeV: JHEP 10 (2018) 167

Bjorken-x



ALI-PREL-502234

Dissociative J/ψ in p-Pb at $\sqrt{s_{NN}} = 8.16$ TeV

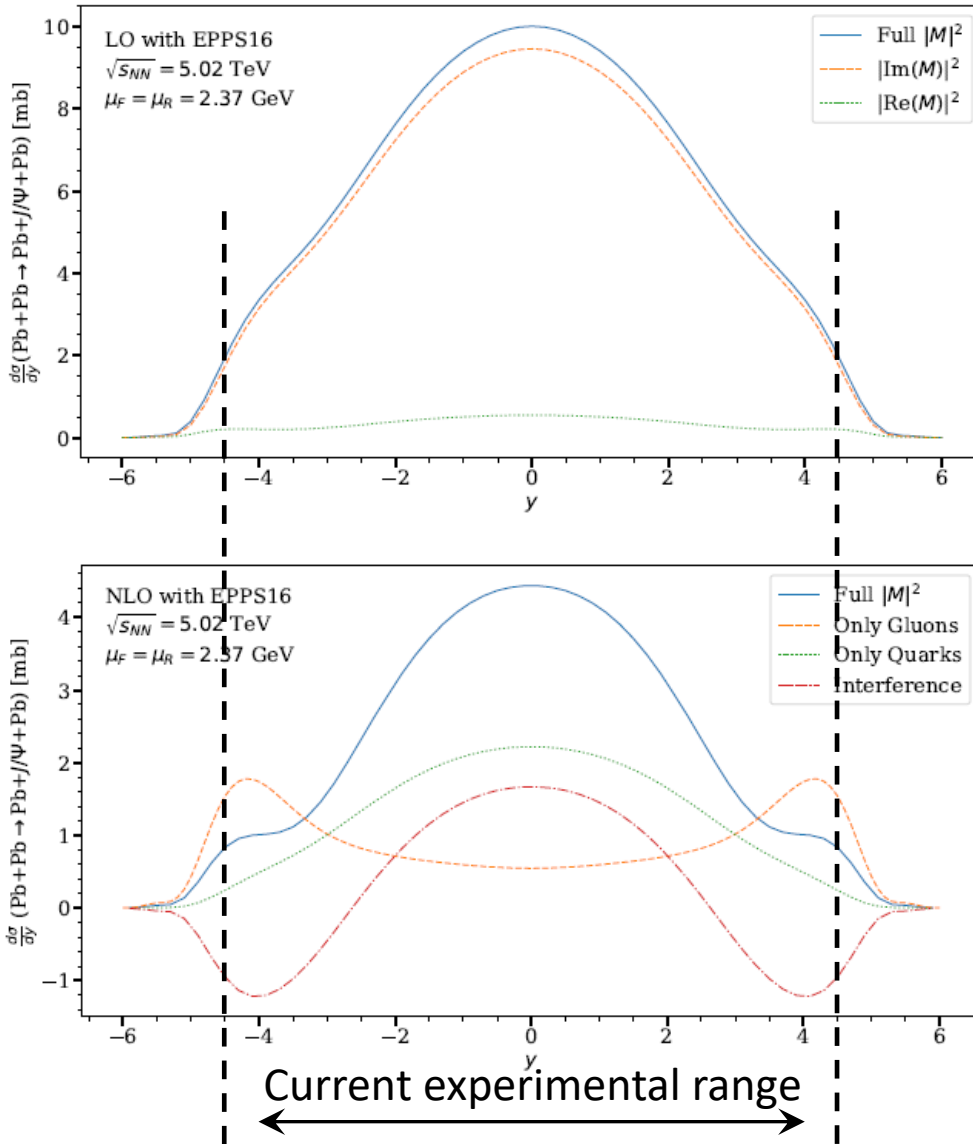


ALI-PREL-502230

ALI-PREL-502226

- **First measurement** of the dissociative cross section at the LHC
- Energy dependent **dissociative J/ψ cross section** ($x_B \sim (0.5, 2) \times 10^{-2}$)
- Agreement with HERA results
- CCT model with saturation agrees with data
 - Predicted maximum at $W_{\gamma p} \sim 500$ GeV to be checked in Run 3
- BM: perturbative JIMWLK evolution with parameters constrained to H1 data to be checked in Run 3

J/ψ photoproduction – LO vs NLO



- LO:
 - Gluons
 - Ryskin, Z. Phys. C 57, 89-92 (1993)

$$\frac{d\sigma(\gamma p \rightarrow J/\psi p)}{dt} = |F^{2G}_N(t)|^2 \frac{\alpha_s^2 \Gamma_{ee}^J m^3_J}{3\alpha_{em}} \pi^3 \left[xG(x, q^2) \frac{2q^2 |q_t^J|^2}{(2q^2)^3} \right]^2$$

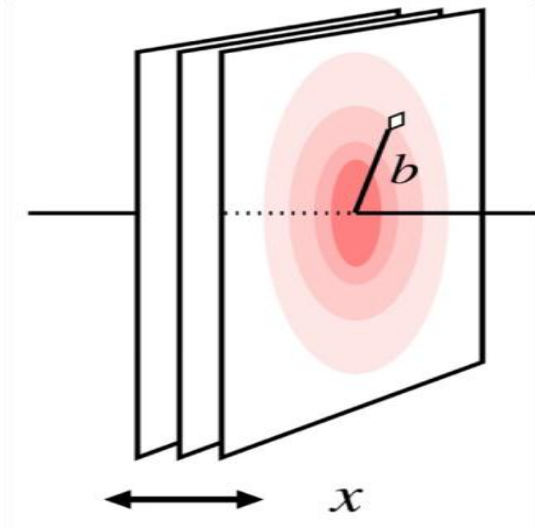
- NLO:
 - Quarks play a role
 - Eskola et al., Phys. Rev. C 106 (2022) no. 3, 035202; arXiv:2210.16048

$$\mathcal{M} = \mathcal{M}_G^{\text{LO}} + \mathcal{M}_G^{\text{NLO}} + \mathcal{M}_Q^{\text{NLO}}$$

- Differences:
 - Gluons vs quarks
 - Shape
 - Normalization
 - Scale dependence
 - nPDF dependence
- What is the impact of higher order corrections?
- Be careful with interpretation!

Motivation for t -dependent measurements

- Gluon density is impact parameter b dependent at given Bjorken- x and Q^2
- b and p_T are Fourier conjugates
- $p_T^2 \approx |t|$ - dependence of the cross section helps to constrain **transverse gluonic structure** at low x_B
- In Good – Walker approach
 - **Coherent** photoproduction tells about **transverse dependence of the gluon shadowing**
 - Saturation may contribute to nuclear shadowing
 - **Incoherent** photoproduction is sensitive to the **variance of the spatial gluon distribution** (subnucleonic fluctuations)



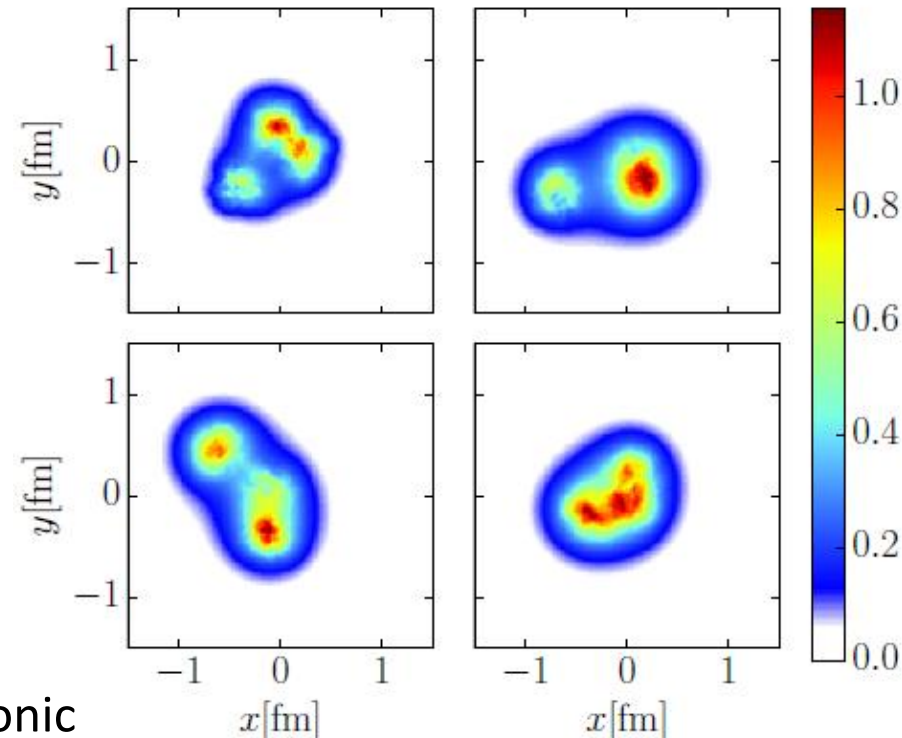
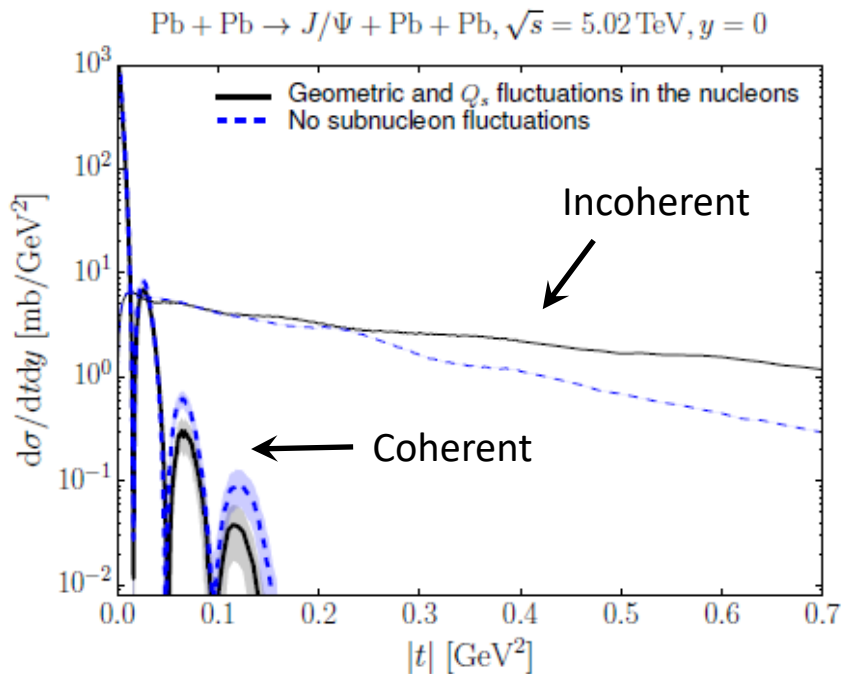
$$\frac{d\sigma^{inc}}{dt} = \frac{Rg^2}{16\pi} (\underbrace{\langle |A(x, Q^2, \vec{\Delta})|^2 \rangle}_{\text{Total}} - \underbrace{|\langle A(x, Q^2, \vec{\Delta}) \rangle|^2}_{\text{Coherent}})$$

Total

Coherent

Motivation – cont.

Mantysaari, Schenke, PLB 772 (2017) 832



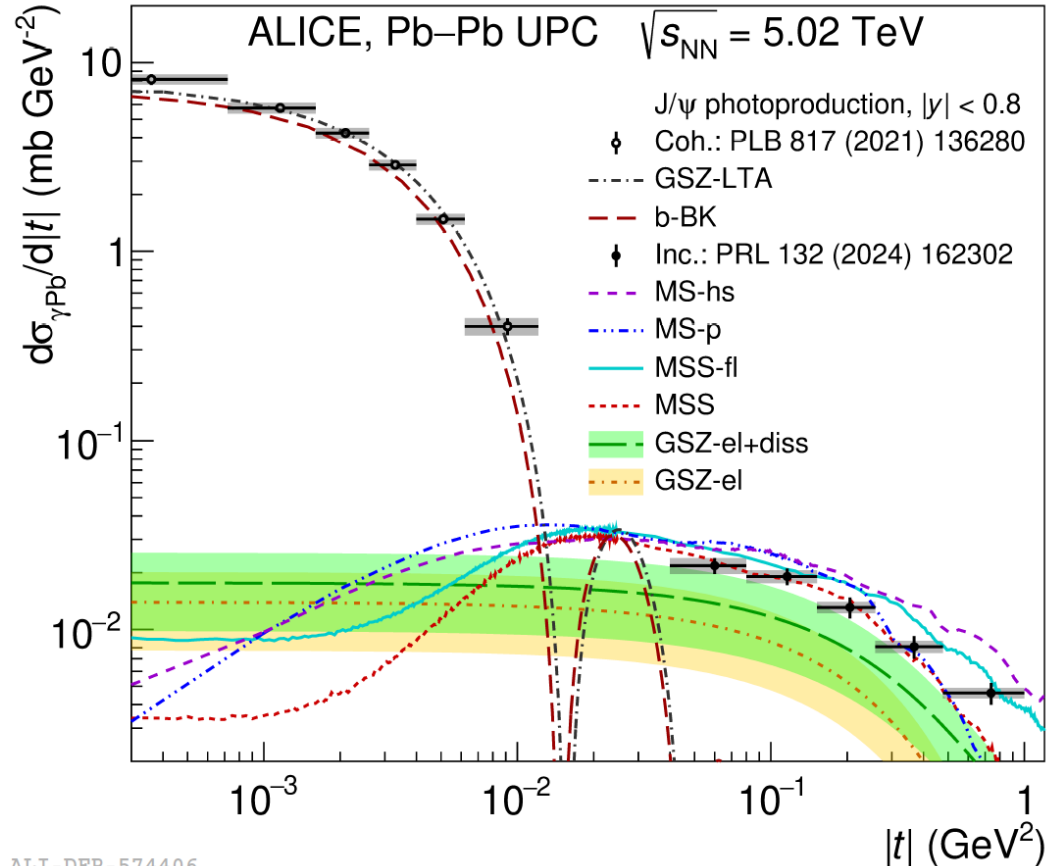
Event by event fluctuations of proton density profile

H. Mantysaari, B. Schenke, PRD 94 (2016) 034042,
 J. Cepila, et al., PLB 766, 186 (2017),
 S. R. Klein, PRC 107, 055203 (2023).

- Variations in nucleon positions and/or gluonic hot spots → **quantum fluctuations**
- Larger $|t|$ range → scatter of smaller object
- Coherent vs. Incoherent vs. Dissociative J/ψ
 - Access to **different scales**: nucleus, nucleon, hot spots

Coherent and incoherent J/ψ - $|t|$

- Gluon density is impact parameter b dependent at given Bjorken- x and Q^2
- b and p_T are Fourier conjugates
- $p_T^2 \approx |t|$ - dependence of cross section constrains transverse gluonic structure at low x_B
- In Good-Walker approach
 - Coherent photoproduction is sensitive to the average spatial gluon distribution
 - Incoherent photoproduction is sensitive to the variance of the spatial gluon distribution (quantum fluctuations)
- Larger $|t|$ range \rightarrow scatter of smaller object



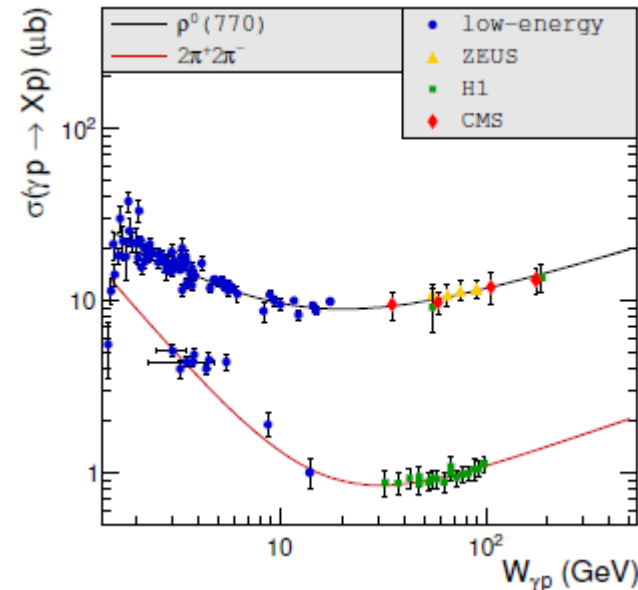
ALI-DER-574406

$$\frac{d\sigma^{inc}}{dt} = \frac{Rg^2}{16\pi} (\langle |A(x, Q^2, \vec{\Delta})|^2 \rangle - |\langle A(x, Q^2, \vec{\Delta}) \rangle|^2)$$

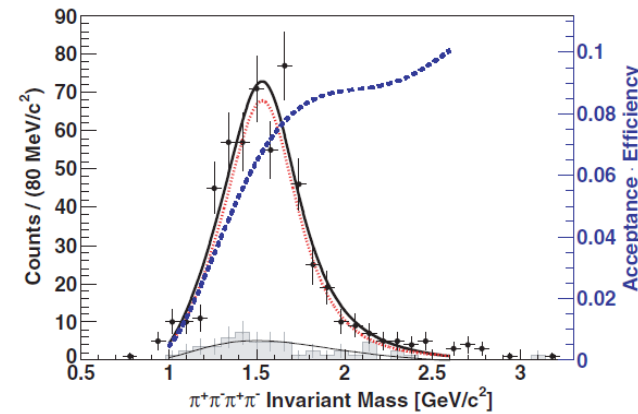
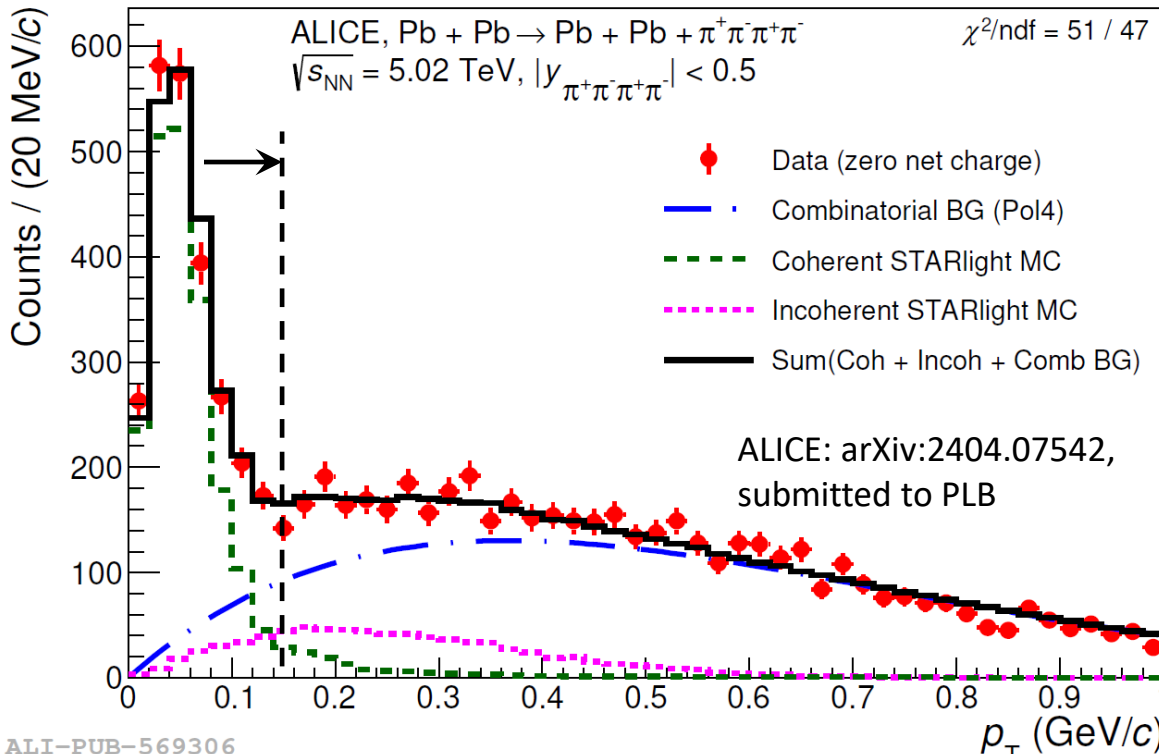
(Slope of) data favor models with gluonic subnucleon fluctuations (hot spots in MS-hs, fluctuations MSS-fl and dissociation in GSZ el+dis)

Exclusive four pion photoproduction

- $\rho^0(770)$ photoproduction extensively studied in H1, ZEUS, STAR, CMS and ALICE
- Excited ρ states expected
 - The mass and the width poorly measured
- $Pb\ Pb \rightarrow Pb\ Pb\ \pi^+\ \pi^-\ \pi^+\ \pi^-$
- Coherent component clearly seen

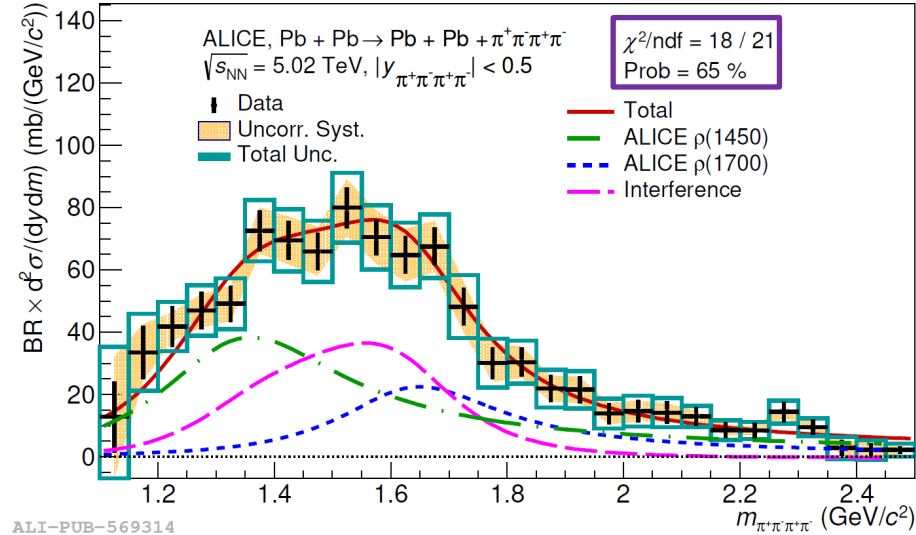
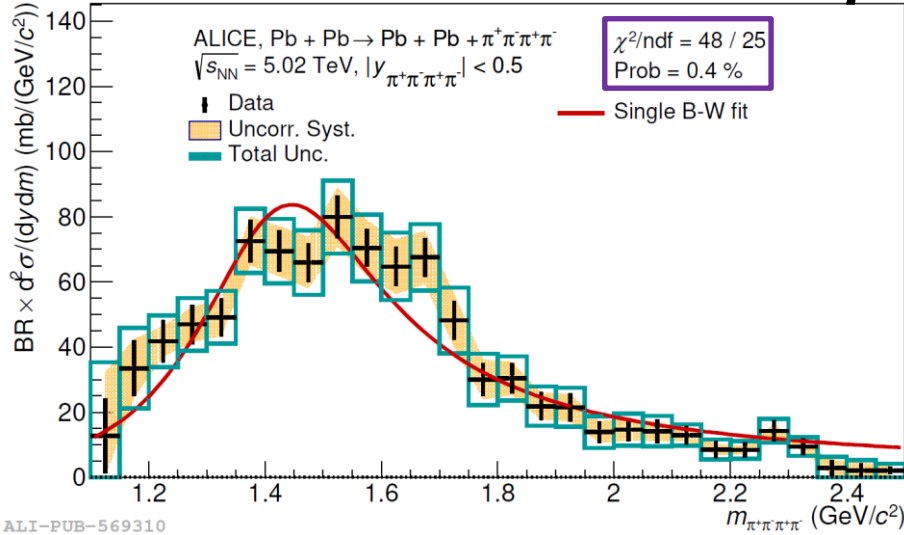


Klusek-Gawenda and Tapia Takaki, Acta Phys. Polon. B51, 6, 1393 (2020)



STAR: PRC 81 044901 (2010)
 $M = 1540 \pm 40$ MeV, $\Gamma = 570 \pm 60$ MeV

Excited ρ resonances



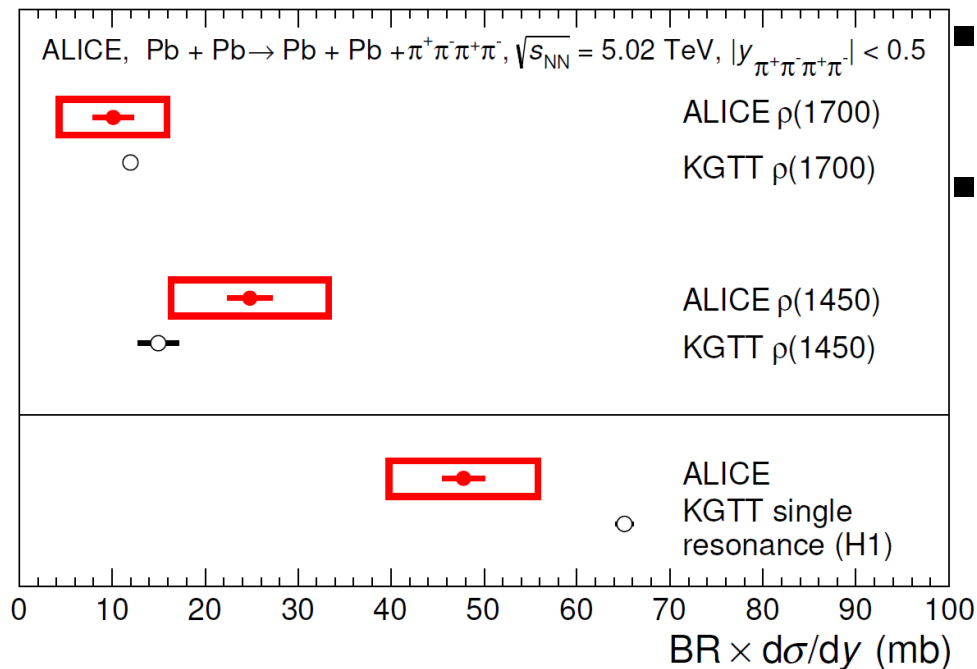
- Fully corrected invariant mass distribution fitted with a relativistic Breit-Wigner with a Söding term with one or two resonances
 - Single resonance fit in agreement with $\rho(1450)$
 - Disfavoured ($\chi^2/\text{ndf} = 48/25$)
 - Two resonances fit give better description ($\chi^2/\text{ndf} = 18/21$)
 - Rough agreement with PDG $\rho(1450)$ and $\rho(1700)$ with mixing angle

	m (MeV/c ²)	Γ (MeV/c ²)
PDG $\rho(1450)$	1465 ± 25	400 ± 60
PDG $\rho(1700)$	1720 ± 20	250 ± 100
STAR Au–Au	1540 ± 40	570 ± 60
ALICE Pb–Pb single resonance	$1463 \pm 2 \pm 15$	$448 \pm 6 \pm 14$
ALICE Pb–Pb $\rho(1450)$	$1385 \pm 14 \pm 36$	$431 \pm 36 \pm 82$
ALICE Pb–Pb $\rho(1700)$	$1663 \pm 13 \pm 22$	$357 \pm 31 \pm 49$
Mixing angle	$1.52 \pm 0.16 \pm 0.19$ (rad)	

$$\frac{d\sigma}{dm_{\pi\pi\pi\pi}} = \left| A \cdot BW_1 + e^{-i\phi} B \cdot BW_2 \right|^2$$

Cross section \times Branching ratio

- Total cross section based on single and double resonance scenario



- Single resonance:
 - $\rho(1450)$: $47.8 \pm 2.3^{stat} \pm 7.7^{syst}$ mb
- Double resonance:
 - $\rho(1450)$: $24.8 \pm 2.5^{stat} \pm 8.1^{syst}$ mb
 - $\rho(1700)$: $10.1 \pm 2.3^{stat} \pm 5.3^{syst}$ mb

KGTT: Acta Phys. Polon. B51, 6, 1393 (2020)

9318 ALICE: arXiv:2404.07542, submitted to PLB

- The sum of cross sections is smaller than the total one due to large interference component
- Cross sections in double resonance scenario give better agreement with theoretical calculations (KGTT) than single resonance scenario

Articles

ALICE

- Coherent J/ψ photoproduction in ultra-peripheral Pb–Pb collisions at $\sqrt{s_{NN}} = 2.76$ TeV, Phys. Lett. B718 (2013) 1273.
- Charmonium and $e + e -$ pair photoproduction at mid-rapidity in ultra-peripheral Pb–Pb collisions at $\sqrt{s_{NN}} = 2.76$ TeV, Eur. Phys. J. C73, 2617 (2013).
- Exclusive J/ψ photoproduction off protons in ultra-peripheral p-Pb collisions at $\sqrt{s_{NN}} = 5.02$ TeV, Phys. Rev. Lett. 113 (2014) 232504.
- Coherent J/ψ photoproduction at forward rapidity in ultra-peripheral Pb-Pb collisions at $\sqrt{s_{NN}} = 5.02$ TeV, Phys.Lett. B798 (2019) 134926.
- Coherent J/ψ and ψ' photoproduction at midrapidity in ultra-peripheral Pb-Pb collisions at $\sqrt{s_{NN}} = 5.02$ TeV, Eur. Phys. J. C 81 (2021) 712.
- First measurement of the $|t|$ -dependence of coherent J/ψ photonuclear production, PLB 817 (2021) 136280.
- Energy dependence of exclusive J/ψ photoproduction off protons in ultra-peripheral p-Pb collisions at $\sqrt{s_{NN}} = 5.02$ TeV, Eur. Phys. J. C (2019) 79: 402.
- Photoproduction of low- p_T J/ψ from peripheral to central Pb-Pb collisions at 5.02 TeV, arXiv:2204.10684 (2022).
- Coherent photoproduction of ρ^0 vector mesons in ultra-peripheral Pb-Pb collisions at $\sqrt{s_{NN}} = 5.02$ TeV, JHEP 06 (2020) 035.
- First measurement of coherent ρ^0 photoproduction in ultra-peripheral Xe-Xe collisions at $\sqrt{s_{NN}} = 5.44$ TeV, Phys. Lett. B 820 (2021) 136481.

CMS

- Coherent J/ψ photoproduction in ultra-peripheral PbPb collisions at $\sqrt{s_{NN}}=2.76$ TeV with the CMS experiment, Physics Letters B772 (2017) 489–511.
- Measurement of exclusive Υ photoproduction from protons in pPb collisions at $\sqrt{s_{NN}} = 5.02$ TeV, Eur. Phys. J. C (2019) 79:277.
- Measurement of exclusive $\rho(770)^0$ photoproduction in ultraperipheral pPb collisions at $\sqrt{s_{NN}} = 5.02$ TeV, Eur. Phys. J. C 79, 702 (2019).

LHCb

- Updated measurements of exclusive J/ψ and $\psi(2S)$ production cross-sections in pp collisions at $\sqrt{s} = 7$ TeV, J. Phys. G 41 (2014) 055002.
- Measurement of the exclusive Υ production cross-section in pp collisions at $\sqrt{s} = 7$ TeV and 8TeV, JHEP 09 (2015) 084.
- Central exclusive production of J/ψ and $\psi(2S)$ mesons in pp collisions at $\sqrt{s} = 13$ TeV, JHEP 10 (2018) 167.
- Study of coherent J/ψ production in lead-lead collisions at $\sqrt{s_{NN}} = 5$ TeV, arXiv:2107.03223v1 [hep-ex] (2021).
- Study of the coherent charmonium production in ultra-peripheral lead-lead collisions, arXiv:2206.08221 [hep-ex] (2022).
- J/ψ photo-production in Pb-Pb peripheral collisions at $\sqrt{s_{NN}} = 5$ TeV, Phys. Rev. C105 (2022) L032201.

Techniques to solve the x_B ambiguity

- Different breakup classes using the neutron ZDC on the A and C side
 - Guzey et al., Eur. Phys. J. C 74 (2014) 7, 2942
 - Photon flux depends on the impact parameter
 - Taken from theory, burdened with uncertainties
 - Solving the linear equations resolves the two-fold ambiguity for VMs at $y \neq 0$

$$\frac{d\sigma_{PbPb}}{dy} = \frac{d\sigma_{PbPb}^{0N0N}}{dy} + 2\frac{d\sigma_{PbPb}^{0NXN}}{dy} + \frac{d\sigma_{PbPb}^{XNXN}}{dy}$$

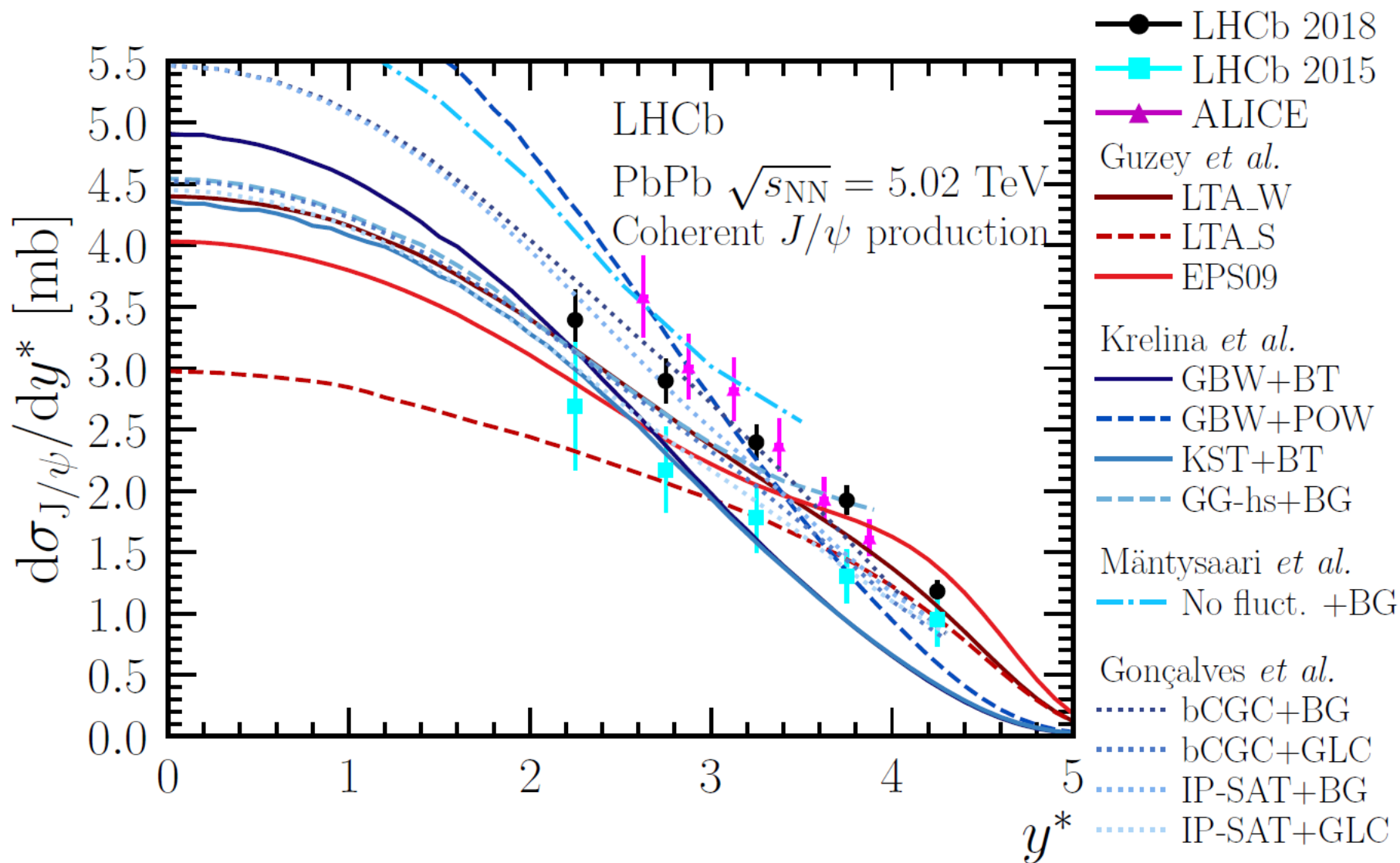
$\frac{d\sigma_{PbPb}^{0N0N}}{dy}$	=	$N^{0N0N}(\omega_{\gamma 1}, +y)\sigma_{\gamma Pb}(\omega_{\gamma 1}, +y) + N^{0N0N}(\omega_{\gamma 2}, -y)\sigma_{\gamma Pb}(\omega_{\gamma 2}, -y)$	
$\frac{d\sigma_{PbPb}^{0NXN}}{dy}$	=	$N^{0NXN}(\omega_{\gamma 1}, +y)\sigma_{\gamma Pb}(\omega_{\gamma 1}, +y) + N^{0NXN}(\omega_{\gamma 2}, -y)\sigma_{\gamma Pb}(\omega_{\gamma 2}, -y)$	extracted
measured		theory	

- Simultaneously uses UPC and peripheral classes
 - Contreras, PRC 96 (2017) 015203

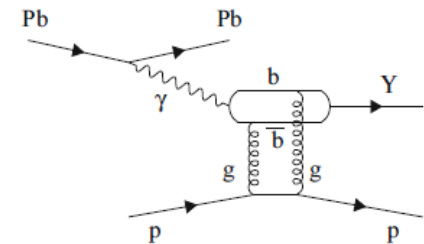
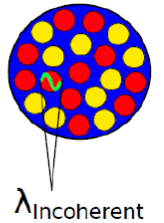
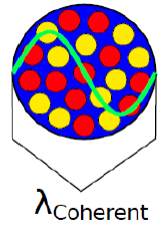
$$\frac{d\sigma_{PbPb}^P}{dy} = N^P(\omega_{\gamma 1}, +y)\sigma_{\gamma Pb}(\omega_{\gamma 1}, +y) + N^P(\omega_{\gamma 2}, -y)\sigma_{\gamma Pb}(\omega_{\gamma 2}, -y)$$

$$\frac{d\sigma_{PbPb}^U}{dy} = N^U(\omega_{\gamma 1}, +y)\sigma_{\gamma Pb}(\omega_{\gamma 1}, +y) + N^U(\omega_{\gamma 2}, -y)\sigma_{\gamma Pb}(\omega_{\gamma 2}, -y)$$

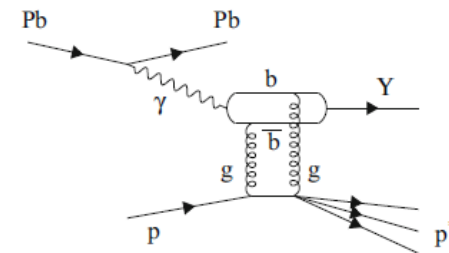
Comparison LHCb/ALICE – Pb-Pb @ 5 TeV



Photoproduction types



Eur. Phys. J. C (2019) 79:277



- **Coherent** Vector Meson (VM) photoproduction:
 - Photon couples coherently to all nucleons (whole nucleus)
 - $\langle p_T^{VM} \rangle \sim 1/R_{pb} \sim 50$ MeV/c
 - Target ion stays intact
- **Incoherent** VM photoproduction:
 - Photon couples to a single nucleon
 - $\langle p_T^{VM} \rangle \sim 1/R_p \sim 400$ MeV/c
 - Target ion breaks, nucleon stays intact
 - Usually accompanied by neutron emission
- **Exclusive** VM photoproduction on target proton:
 - Photon couples to a single proton
 - $\langle p_T^{VM} \rangle \sim 1/R_p \sim 400$ MeV/c
 - Target proton stays intact (similar to coherent) in p-Pb case
- **Dissociative** (or semiexclusive) VM photoproduction:
 - Photon interacts with a single nucleon and excites it
 - $\langle p_T^{VM} \rangle \sim 1$ GeV/c
 - Target nucleon and ion break (in heavy ion collision)
 - Target proton breaks (in p-Pb)